의학박사 학위논문

골격근에서 지방 대사에 대한 SENP2 의 역할

Role of SENP2 on lipid metabolism in skeletal muscle

2016 년 2 월

서울대학교 대학원

의과학과 의과학전공

구 영 도

Role of SENP2 on lipid metabolism in skeletal muscle

골격근에서 지방 대사에 대한 SENP2 의 역할

February 2016

The Department of Biomedical Sciences,

Seoul National University

College of Medicine

Young Do Koo

골격근에서 지방 대사에 대한 SENP2 의 역할

지도교수 이 동 섭

이 논문을 의학박사 학위논문으로 제출함

2015 년 10 월

서울대학교 대학원

의과학과 의과학전공

구 영 도

구영도의 의학박사 학위논문을 인준함

2015 년 12 월

위 원 장 _____ (인)

부위원장 _____ (인)

위 원 _____ (인)

위 원 _____ (인)

위 원 _____ (인)

Role of SENP2 on lipid metabolism in skeletal muscle

by

Young Do Koo

A thesis submitted to the Department of Biomedical Sciences in partial fulfillment of the requirements for the Degree of Doctor of Philosophy in Medicine at Seoul National University College of Medicine

December 2015

Approved by Thesis Committee

Professor _____ Chairman

Professor _____ Vice Chairman

Professor _____

Professor _____

Professor _____

Abstract

SUMO modification (SUMOylation) is a posttranslational modification of protein, which is a reversible process. SUMOylation of proteins has many functions. Many papers reported protein stability, transcriptional regulation, and nuclear-cytosolic transport by SUMOylation. Typically, small fraction of protein is SUMOylated and this modification is rapidly reversed by the action of deSUMOylating enzymes. deSUMOylation is catalyzed by SUMO-specific proteases (SENPs). However, the physiological function of SENPs in energy metabolism remains unclear. In this study, I investigated the role of SENP2 in fatty acid metabolism in C2C12 myotubes and SENP2 skeletal muscle specific transgenic mouse models.

When C2C12 myotubes were treated with palmitate, expression of SENP2 was increased via TLR4-Myd88-NF-κB signaling pathway. This increase promoted the recruitment of PPARδ and PPARγ, through deSUMOylation of PPARs, to the promoters of the genes involved in fatty acid oxidation (FAO), such as carnitine-palmitoyl transferase-1 (CPT1b) and long-chain acyl-CoA synthetase 1 (ACSL1). In addition, SENP2 induced by palmitate increased levels of fatty acid oxidation in C2C12 myotubes. When PPARδ, PPAR or SENP2 were silenced, palmitate does not increase fatty acid oxidation and

expressions of fatty acid oxidation associated genes.

When C2C12 myotubes were transfected with SENP2 adeno viruses, fatty acid oxidation levels were increased. Expression levels of fatty acid oxidation associated genes, such as CPT1b and ACSL1, were increased by SENP2 in C2C12 myotubes. SENP2 skeletal muscle specific transgenic FVB (SENP2 TG) mice showed significant improvement of glucose tolerance, insulin resistance, body weight and fat mass in a high fat diet condition. Also, β-oxidation and mitochondrial mass are increased in mouse skeletal muscle tissue of SENP2 TG mice. Furthermore, Insulin signaling pathway-related genes were up-regulated by SENP2 overexpression in skeletal muscle tissue.

In summary, these results indicate that SENP2 plays an important role in fatty acid metabolism and mitochondrial biogenesis in skeletal muscle. Furthermore, SENP2 could be a novel therapeutic target for the treatment of obesity-linked metabolic disorders.

Keywords : SENP2, deSUMOylation, Fatty acid metabolism,

Obesity, Skeletal muscle

Student Number : 2009-30599

Contents

Abstract

List of figure

Chapter I. Regulation of SENP2 by palmitate via NF-κB signaling pathway

Introduction

Material and Method

Results

Discussion

Chapter II. Control of fatty acid metabolism by SENP2 overexpression

Introduction

Material and Method

Results

Discussion

References

국문초록

List of figures and Tables

Table 1. Primer sequences

Figure 1. Palmitate increases SENP2 mRNA levels in C2C12 myotubes

Figure 2. Palmitate increase SENP2 expression levels, in a time- and dose- dependent manner

Figure 3. Palmitate has no effect on SENP1 expression levels

Figure 4. Palmitate increases SENP2 expression via NF-κB activation in C2C12 myotubes

Figure 5. Knockdown of NF-κB inhibits palmitate-induced SENP2 in C2C12 myotubes

Figure 6. Palmitate increases SENP2 expression via NF-κB activated by TLR4 and Myd88 signaling

Figure 7. Palmitate increases binding of NF-κB to SENP2 promoter region

Figure 8. Palmitate up-regulates expression FAO-related genes in a dose-dependent manner

Figure 9. FAO is increased by palmitate via SENP2

Figure 10. Palmitate-induced increase of mRNA levels of FAO-related genes is mediated by SENP2

Figure 11. Up-regulation of SENP2 by palmitate leads to binding of PPARδ and PPARγ on promoter regions of CPT1b and ACSL1 genes

Figure 12. Regulation of SENP2 by fatty acid in the skeletal muscle

Figure 13. Microarray analysis

Figure 14. SENP2 increases FAO and expression of FAO-related genes in C2C12 myotubes

Figure 15. Expression levels of transcription factors by SENP2 overexpression

Figure 16. FAO and mRNA levels of FAO-related genes are increased by SENP2 via PPARδ and PPARγ

Figure 17. Knock-down of transcription factors does not change the basal FAO levels

Figure 18. Binding of PPARδ and PPARγ to the promoter regions of the FAO-related genes is increased by SENP2

Table 2. PPARδ has a SUMOylation site

Figure 19. PPARδ is deSUMOylated by SUMO1

Figure 20. PPARδ is deSUMOylated by SENP2

Figure 21. SUMOylation of PPARδ may promotes ubiquitination

Figure 22. SENP2 stimulates deSUMOylation of endogenous PPARδ in C2C12 myotubes

Figure 23. deSUMOylation of PPARδ by SENP2 increases transcriptional activity of PPARδ

Figure 24. Plasmid construct for skeletal muscle SENP2 transgenic (mSENP2-TG) mice

Figure 25. Comparison of SENP2 expression levels in both WT and mSENP2 TG mice

Figure 26. SENP2 overexpression decreases fat mass and body weight, but does not have an effect on lean mass and bone mineral content

Figure 27. Glucose tolerance and insulin resistance are improved by SENP2

Figure 28. Serum analysis of WT and mSENP2-TG mice in chow and high fat diet (HFD) conditions

Figure 29. SENP2 overexpression decreases lipid accumulation and increases mitochondria biogenesis

Figure 30. H&E staining analysis of liver and white adipose tissue of WT and mSENP2-TG mice

Figure 31. SENP2 improves insulin signaling pathway

Figure 32. SENP2 increases ATP contents in HFD conditions

Figure 33. The levels of FFA and triglyceride in gastrocnemius muscle.

Figure 34. SENP2 increases fatty acid oxidation (FAO) in skeletal muscle tissue.

Figure 35. Effects of SENP2 overexpression on RNA levels of various genes in skeletal muscle

Figure 36. Control of fatty acid metabolism by SENP2 overexpression

Chapter I.

Regulation of SENP2 by fatty acid

in skeletal muscle

Introduction

Type 2 diabetes mellitus (T2DM) is one of the most rapidly growing diseases and develops as a combined consequence of insulin resistance and relative insulin deficiency. Type 2 diabetes (T2D) is characterised by resistance to the action of insulin in key metabolic tissues such as skeletal muscle, liver and adipose tissue, coupled with reduced insulin secretion caused by impaired β-cell function in the pancreas [1]. Also, Insulin resistance is associated with dysfunction of mitochondria related with accumulation of excess lipids. Energy expenditure is very important to maintain normal body weight. Body weight reflects the balance between energy intake and consumption [2]. Skeletal muscle is a major organ for energy expenditure related fatty acid oxidation in mitochondria and a primary site of insulin-stimulated glucose uptake [3-5]. Furthermore, skeletal muscles are essential for postural maintenance, locomotion and respiration, and require high amounts of ATP during contractions. Mitochondria are the major site of oxidative metabolism to generate ATP and reactive oxygen species (ROS) [6-10]. To limit oxidative stress, ROS generation is counterbalanced by the action of anti-oxidant enzymes [11]. Consequently, dysregulation of energy metabolism in skeletal muscle leads to metabolic

disorder.

Peroxisome proliferator-activated receptors (PPARs) are members of the nuclear receptor superfamily including PPARα, PPARδ and PPARγ. These receptors bind to and are activated by a number of drugs used in the treatment of hyperlipidemia and T2DM [12, 13]. PPARα is expressed most in brown adipose tissue and liver. PPARδ is found in many tissues and highly expressed in the skeletal muscle for lipid metabolism. PPARγ is mainly expressed in adipose tissue and plays an essential role in adipogenesis.[14, 15] The mechanism of transcriptional regulation by PPARs is complex because it activates or represses transcription by recruiting coactivator or corepressor complexes to various target gene promoters.[12] PPARs play roles in lipid and fatty acid metabolism by directly binding to and modulating genes involved in fat metabolism [16, 17]. PPARγ is known as a key regulator for adipocyte differentiation and does not seem to be involved with oxidative metabolism [18]. PPARα and PPARδ are essential regulators of fatty acid oxidation (FAO) [19, 20]. PPARα in FAO regulation is expressed in the heart, liver and brown adipose tissue [21]. On the other hand, PPARδ is ubiquitously expressed with higher levels in the digestive tract, heart, brown adipose tissue and skeletal muscle [22].

SUMO (small ubiquitin-like modifier) modulates many processes such as

nuclear transport, transcription replication, recombination and chromosome segregation [23, 24]. Conjugation results in formation of isopeptide bond between c-terminus of SUMO and e-amino group of a lysine within target protein. Enzymes responsible for SUMO processing and deconjugation are called Ubl (ubiquitin-like protein)-specific proteases (Ulp) in yeast [25] and Sentrin-specific proteases (SENP) in mammals [26]. SUMO functions in a manner similar to ubiquitin, where it is bound to target proteins as part of a post-translational modification system. Similar to ubiquitination, SUMOylation requires processing, conjugation and transfer. The transfer process is catalyzed by E3 ligases [27]. The reverse deSUMOylation process is mediated by SUMO-specific proteases (SENPs). SENP1, SENP2, SENP3 and SENP5 are originated from the Ulp1 branch. SENP1 and SENP2 are closely related to each other, and both localize within the cell at the nuclear envelope through association to the nuclear pore complex (NPC) [28-30]. Similarly, SENP3 and SENP5 show the highest degree of homology with each other and share a common localization to nucleoli [31-33]. SENP6 and SENP7 fall within the Ulp2 branch, and both localize to the nucleoplasm [34].

Some papers reported that relation of PPARs and SUMOylation was very important. Stability and transcription activity of PPARγ2 are controlled by

SUMOylation and deSUMOylation [35-37]. The ability of PPARγ agonists to antagonize inflammatory responses by repression of nuclear factor kappa B (NF-kB) target genes is linked to anti-diabetic [38] and anti-atherogenic effects [39]. NCoR and the related factor SMRT (silencing mediator of retinoic acid and thyroid hormone receptors) are components of corepressor complexes containing HDAC3. NCoR/SMRT complexes are also required for basal repression of a subset of NF-kB and AP-1 target genes [40-42]. SUMOylation of PPARγ promotes interaction with the NCoR–HDAC3 complex [43]. KLF5, PPARδ and corepressors, such as NCoR and SMRT, bind to promoters of lipid metabolism associated genes. Dissociation of corepressors and KLF5 by SENP1 increase expression of lipid metabolism associated genes [44]. PPARγ has domains for NF-κB inhibition and SUMOylation of PPARγ prevents the removal of NCoR from NF-κB binding sites of pro-inflammatory genes [45].

It is known that SENPs has important role in tumor growth [46, 47], alzheimer's disease [48, 49] and metabolic disease [50-52] etc. SENP2 catalyzes the deSUMOylation process of Mdm2. SENP2-dependent regulation of Mdm2 is sensitive to its p53-binding activity in human colorectal carcinoma cell line [46]. The Pin1 regulates phosphorylation signaling by controlling protein conformation after phosphorylation, and its

upregulation promotes oncogenesis via acting on numerous oncogenic molecules. Pin1 is SUMOylated by SUMO1 and is deSUMOylated by SENP1. deSUMOylated Pin1 by SENP1 control it's activity and cellular functions [47]. Pancreatic islet–specific knockout of SENP1 attenuates insulin secretion due to an impaired amplification of exocytosis [51]. Also, our lab recently shown that SENP2 deSUMOylates PPARγ and dramatically increases it's activity in adipocyte and skeletal muscle cell lines. In adipocytes, SUMOylation of C/EBPβ dramatically increased its ubiquitination and destabilization, and this increase could be reversed by SENP2 [53]. Interestingly, the SUMOylation of PPARγ selectively regulates the expression of some PPARγ target genes in myotubes, and deSUMOylates of PPARγ increases the mRNA level of fatty acid translocase [54].

As mentioned above, I hypothesized that SENP2 is involved in metabolic regulation in skeletal muscle. So, I tried to understand the regulation mechanism of SENP2 in the skeletal muscle.

Material and method

Cell culture

C2C12 myoblasts were maintained in DMEM supplemented with 10% FBS (Invitrogen, MA, USA). Differentiation was induced using DMEM containing 2% horse serum (Invitrogen, MA, USA) for 4 days. Transfection of plasmids was performed using Lipofectamin with Plus Reagent (Invitrogen, MA, USA), and siRNAs were transfected using RNAiMAX (Invitrogen, MA, USA) for 3 days before cell harvest. COS7 cells were maintained in DMEM supplemented with 10% FBS (Invitrogen, MA, USA).

siRNA treatment

Small interfering RNAs (siRNAs) of TLR4, Myd88, NF-κB and SENP2 were purchased from Dhamacon (Chicago, IL, USA) and nonspecific siRNAs (negative control) were purchased from BIONEER (Daejeon, Korea). 50 nM of siRNA or siNS was mixed with RNAiMAX (Invitrogen, MA, USA) in 100 μl of serum-free DMEM and incubated for 30 min at room temperature. The complex was treated to the cells with 400 μl of serum-free DMEM. After 4hour incubation, 500 μl of DMEM media supplemented with

2% horse serum were added.

RNA preparation and Real-time PCR

Total RNAs of differentiated C2C12 cells were isolated using TRIzol (Invitrogen, MA, USA) according to the manufacturer's instruction. To prepare cDNA, 10μl of reaction buffer (Invitrogen, MA, USA), 5 μl of 100 mM DTT, 2.5 μl of 10mM dNTP, 1 μl of Oilgo dT, 0.5μl of RNase inhibitor, 2 μl of RTase and 1 μg of RNA were mixed and RNase free water was added up to 50 μl. The mixture was incubated at 37°c for 1 hour and at 72°c for 10 min using PCR system. Expression levels of genes were determined by using SYBR-MASTER MIX (Takara, Otsu, Shiga, Japan) and ABI 7500 Real-time PCR system (Applied Biosystem, CA, USA). The primer sequences for PCR of the genes were as followed table.

Table 1. Primer sequences

	Forward primers	Reverse primers
SENP2	5' GCT GGC TAA GGT TCT CGG C 3'	5' CTG GGA TCT CAT CAG TGT CCA 3'
CPT1b	5' AAG TGT AGG ACC AGC CCC GA 3'	5' TGC GGA CTC GTT GGT ACA GG 3'
ACSL1	5' CTG GTT GCT GCC TGA GCT TG 3'	5' TTG CCC CTT TCA CAC ACA CC 3'
UCP3	5' AGG AGC CAT GGC AGT GAC CT 3'	5' CAC AGG CCC CTG ACT CCT TC 3'
PPARα	5' AGA GCC CCA TCT GTC CTC TC 3'	5' ACT GGT AGT CTG CAA AAC CAA A 3'
PPARδ	5' ACA GAA GGG CCT GGT GTG GA 3'	5' AGA GGC TGC TGA AGT TGG GG 3'
PPARγ	5' GGA AGA CCA CTC GCA TTC CTT 3'	5' TCG CAC TTT GGT ATT CTT GGA G 3'
PGC1α	5' ACC TGA CAC AAC GCG GAC AG 3'	5' TCT CAA GAG CAG CGA AAG CG 3'
ERRα	5' CTC AGC TCT CTA CCC AAA CGC 3'	5' CCG CTT GGT GAT CTC ACA CTC 3'
RIP140	5' CAT CTG CAT GGT CCC GAA GA 3'	5' CCG CTG TGA TGA TTG GCA GT 3'
TLR4	5' TAG AAG AAG GAG TGC CCC GC 3'	5' ACC TTC CGG CTC TTG TGG AA 3'
Myd88	5' AAC TGG GAG GCA TCA CCA CC 3'	5' CCG GAT CAT CTC CTG CAC AA 3'
SENP1	5' CAC TCC AGC GTC AGG CTC AG 3'	5' ATG GAC TTG GGG CAG GCT TA 3'
NFkB	5' AGG ACC CAA GGA CAT GGT GG 3'	5' GTG AGT TGC CGG TCT CCT CC 3'
GAPDH	5' AGG TCG GTG TGA ACG GAT TTG 3'	5' TGT AGA CCA TGT AGT TGA GGT CA 3'
CPT1b (Chip)	5′ GAG CAG CAG TGG TCC CTG AG 3′	5′ TGC TGG AAG GTC TGG GAC TG 3′
ACSL1 (Chip)	5' GGT GAC TCT ACT CTC AGC TGC 3'	5' CTTACCAGGCTGCCAAGGTCT 3'

Western Blotting

Tissues and cells were lysed in 20 mM Tris-HCl, pH 7.4, 10 mM $Na_4P_2O_7$, 100 mM NaF, 2 mM Na_3VO_4, 1% NP-40 buffer supplemented with protease inhibitor (10 μg/μl aprotinin, 10 μg/μl luepeptin and 1mM PMSF). The whole-cell lysates were sonicated 15 seconds for two times, and cell debris was removed by centrifugation (13,000 rpm) for 30 min at 4°c. About 20~30

μg of proteins were separated on the SDS-PAGE. Separated proteins were transferred onto nitrocellulose membrane (Whatman, Dassel, Germany). The membrane was blocked with 5% skim milk in Tween20-Tris-buffered saline (TBS-T) for 1~2 h at room temperature, and it was incubated with the specific primary antibody for overnight at 4°c. Membranes were probed with specific antibodies and bands were visualized by enhanced chemi-luminescence (Pierce, IL, USA).

Measurement of Fatty Acid Oxidation

For measurement of FAO, muscle tissues or cells were homogenized in an ice-cold mitochondria isolation buffer (250 mM sucrose, 10 mM Tris-HCl, and 1 mM EDTA). The lysates were incubated for 2 h with 0.2 mM [1-^{14}C]palmitate. $^{14}CO_2$ and ^{14}C-labeled acid-soluble metabolites were quantified using a liquid scintillation counter. Each radioactivity was normalized by protein amount of each lysate.

Immunoprecipitation

Tissues and cells were prepared with the lysis buffer (20 mM Tris-HCl pH 7.4, 1% Triton X-100, 1% Sodium deoxycholate, 0.1% SDS, 150 mM NaCl,

1 mM EGTA, 10 mM $Na_4P_2O_7$, 100 mM NaF, 2 mM Na_3VO_4, 10 µg/µl aprotinin, 10 µg/µl luepeptin and 1 mM PMSF) (Sigma, St. Louis, MI, USA) for Immunoprecipitation assay. Cell debris was removed by centrifugation for 30 min at 4°c. Protein concentration was determined by Bradford assay (Bio-Rad, Hercules, CA, USA). Lysate (700 µg) were incubated with anti-HA (12CA5) (Roche, Mannheim, Germany) and Protein G Separose (GE Healthcare, Uppsala, Sweden) for overnight at 4°c. The beads were washed twice with the lysis buffer and phosphate-berffered saline (PBS), respectively. The IP samples were eluted in Laemmli sample buffer (62.5 mM Tris-HCl pH 6.8, 2% SDS, 25% glycerol, 5% 2-mercaptoethanol, 0.01% Bromophenol Blue) (Sigma, St. Louis, MI, USA).

Nuclear Extraction

C2C12 myotubes were detached by scrapping and collected in tubes. Then, cells were resuspended in cold PBS and centrifuged. Cell membranes were homogenized with destruct buffer (Hepes 10 mM, KCl 10 mM, $MgCl_2$ 1.5 mM, DTT 0.5 mM) and placed on ice for 10 min. Nuclear pallet was collected by centrifugation (3,300 xg) for 10 min. High salt nuclei lysis buffer (Hepes 20 mM, $MgCl_2$ 1.5 mM, DTT 0.5 mM, EDTA 0. 2mM, NaCl 420 mM, glycerol 25%, PMSF 0.5 mM, Aprotinin 2 µg/ml, Leupeptin 0.7

μg/ml) was added to nuclear pellet. Desalting step was performed by dialysis. Dialysis buffer formula is as follow : Hepes 20 mM, KCl 100 mM, DTT 0.5 mM, EDTA 0.2 mM, NaCl 20 mM, glycerol 25%, PMSF 0.5 mM.

EMSA (Electrophoric Mobility Shift Assay)

Oligonucleotides for NF-κB binding site of SENP2 promoter region (5' – GAA CGT TAA ATC TGT GGG CCC TCT GAT GGC GT – 3', upper strand) and the mutant (5' – GAA CGT TAA ATC TGT CTC CCC TCT GAT GGC GT – 3', upper strand) were used for a probe or competitors. The sequence of consensus NF-κB was AGT TGA GGG GAC TTT CCC AGG. The probe was labeled with biotin using LightShift Chemiluminescent EMSA kit. Mixture of labeled DNA and nuclear extracts from C2C12 myotubes treated with palmitate for 24 h were incubated at room temperature for 30 min. Competitors were added at 50 fold molar excesses to the labeled probe. The incubated mixture samples were separated on 6% polyacrylamide gels.

ChIP (Chromatin Immunoprecipitation)

C2C12 myotubes were transfected with siRNA (50 nM) of SENP2 for 3 days and treated with palmitate (0.5 mM) for 24 h before harvest. After cross-

linking and DNA fragmentation, nuclear extracts were immunoprecipitated with PPARδ and PPARɣ antibodies or control IgG. Primers used for real-time PCR were 5'-GAG CAG CAG TGG TCC CTG AG-3' and 5'-TGC TGG AAG GTC TGG GAC TG-3' for CPT1b-PPRE ; 5'-GGT GAC TCT ACT CTC AGC TGC-3' 5'-CTTACCAGGCTGCCAAGGTCT -3' for ACSL1-PPRE.

Statistical analysis

Statistical analysis was performed using SPSS version 12.0 (SPSS Inc.). Statistical significance was tested using the Mann-Whitney U test. A *P* value below 0.05 was considered statistically significant.

Results

Saturated fatty acid is modulators which increases expression levels of SENP2 in C2C12 myotubes.

Next, I wondered what is regulator of SENP2. For finding the regulator of SENP2 expression, C2C12 myotubes were treated with various metabolites, hormones, and cytokines. The expression of SENP2 mRNA was not significantly changed upon treatment with insulin, rosiglitazone, inerleukin-6 (IL-6), tumor necrosis factor α (TNFα), mitochondrial complex inhibitor (rotenone) or unsaturated fatty acid (oleic acid, linoleic acid, and eicosapentaenoic acid) (Figure 1). However, it was markedly increased by treatment with a saturated fatty acid, palmitate, (Figure 1) and this increase occurred in a dose- and time- dependent manner (Figure 2A, 2B). Also, SENP2 protein levels were increased by palmitate in C2C12 myotubes (Figure 2C). In addition, the expression of SENP1, another SENP, was not influenced by any of the tested fatty acids, including palmitate (Figure 3). These results suggest that palmitate specifically regulates the expression of SENP2 in C2C12 myotubes.

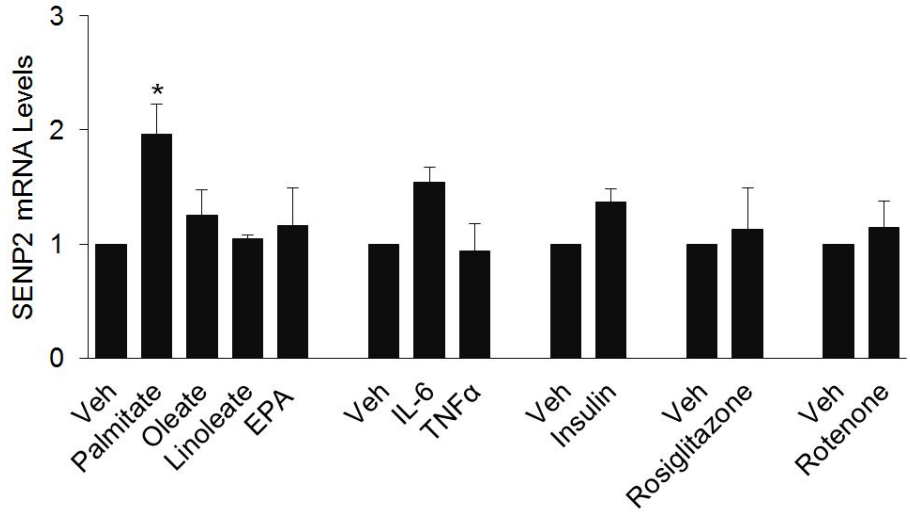

Figure 1. Palmitate increases SENP2 mRNA levels in C2C12 myotubes

C2C12 myotubes were fully differentiated under 2% horse serum in DMEM media. The cells were treated with palmitate (500 μM), oleate (500 μM), linolate (500 μM), EPA (500 μM), IL-6 (50 ng/ml), TNFα (50 ng/ml), insulin (5 unit/ml), rosiglitazone (10 μM) or rotenone (3 μM) for 24 h. Total RNA was extracted from C2C12 myotubes. The RNA (1 μg) subjected to real-time PCR using primers for SENP2. n=7.

(* = $p < 0.05$ *vs* Veh)

(A)

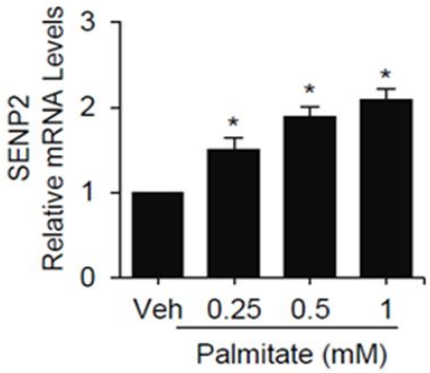
SENP2
Relative mRNA Levels
3
2
1
0
*
*
*
Veh
0.25
0.5
1
Palmitate (mM)

(B)

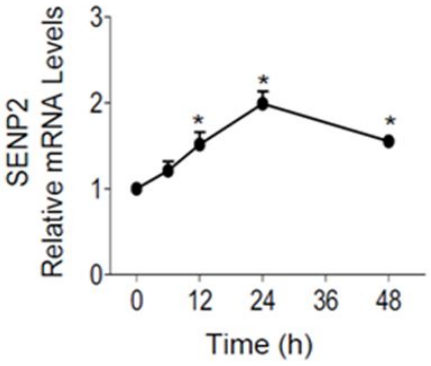
SENP2
Relative mRNA Levels
3
2
1
0
*
*
*
0
12
24
36
48
Time (h)

(C)

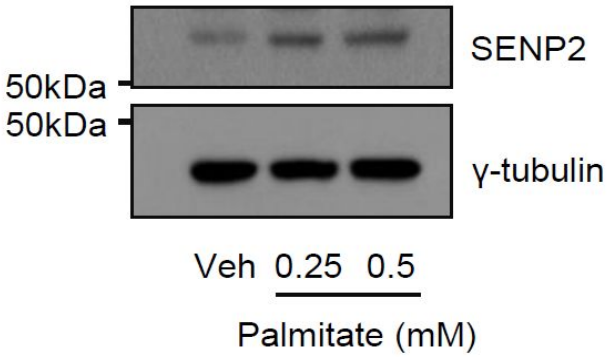
SENP2
50kDa
50kDa
γ-tubulin
Veh
0.25
0.5
Palmitate (mM)

Figure 2. Palmitate increases SENP2 expression levels, in a time- and dose- dependent manner

(A) C2C12 myotubes were treated with 0.25 mM, 0.5 mM or 1 mM of palmitate for 24 h. Palmitate was dissolved in 100% Ethanol. (B) The cells were treated with 0.5 mM of palmitate for 12, 24, 36 or 48h in DMEM supplemented with 1.5% BSA and 2% HS. Total RNA was extracted and subjected to real-time PCR using primers for SENP2. (C) C2C12 myotubes were treated with 0.25 mM, 0.5 mM or 1 mM of palmitate for 24 h. The lysate were subjected to immunoblot with anti-SENP2.

n=6. (* = $p < 0.05$ *vs* Veh)

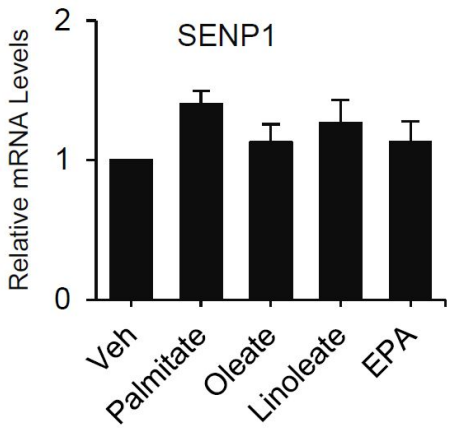

Figure 3. Palmitate has no effect on SENP1 expression levels

C2C12 myotubes were treated with 0.5 mM of palmitate, oleate, linolate or EPA for 24 h (A). Total RNA was extracted from C2C12 myotubes. The RNA (1 μg) subjected to real-time PCR using primers for SENP1. n=6

SENP2 expression is regulated by palmitate-induced* NF-κB *activation

Palmitate is known to induce activation of NF-κB [55, 56]. It has also been shown that toll- like receptor 4 (TLR4) and MyD88 are responsible for palmitate-induced NF-κB activation [56-58]. Treatment with pyrrolidine dithiocarbamate (PDTC), a selective NF-κB inhibitor, abrogated palmitate-mediated increase in the mRNA level of SENP2 (Figure 4). Next, I experimented knockdown of NF-κB by specific siRNAs (Figure 5A) Knock down of NF-κB completely inhibited the effect of palmitate on the SENP2 mRNA level (Figure 5B). Moreover, knockdown of TLR4 or MyD88 (Figure 6A) led to suppression of palmitate-induced expression of SENP2 mRNA (Figure 6B). These results suggest that the increase of the SENP2 mRNA level by palmitate is mediated NF-κB activation via TLR4 and Myd88.

To determine whether the promoter of the mouse SENP2 gene has a cis-acting element for NF-κB-mediated regulation, its 5'-flanking region was serially deleted and inserted into a Luc reporter vector. Palmitate treatment led to 3- to 4-fold increase in the luciferase activity upon transfection of the constructs having the regions from -1980, - 868, and -157 to +93 bp (Figure 7A). Furthermore, a potential NF-κB-binding sequence was found to locate at about 70 bp upstream of the transcription start site and mutations of the sequence abrogated palmitate-induced promoter activity (Figure 7B). To

confirm this finding, I performed electrophoretic-mobility shift assay (EMSA) by using nuclear extracts of C2C12 myotubes (Figure 7C). Palmitate treatment led to a dramatic increase in a binding with a biotin-labeled probe containing the putative NF-κB-binding sequence (Figure 7C, lane 3) and this increased binding could be abolished by treatment with the same but unlabeled probe (Figure 7C, lane 4) as well as with the unlabeled consensus NF-κB-binding sequence (Figure 7C, lane 6), but not with a oligonucleotide having the mutated sequence (Figure 7C, lane 5). Furthermore, the band was super-shifted by addition of anti- NF-κB antibody (Figure 7C, lane 7). These results suggest that the SENP2 promoter has a cis-acting element for palmitate-induced NF-κB binding.

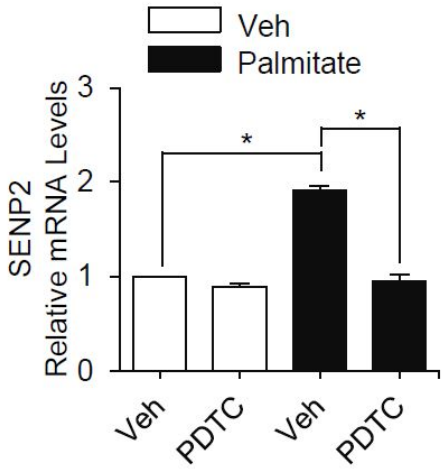

Figure 4. Palmitate increases SENP2 expression via NF-κB activation in C2C12 myotubes

C2C12 myotubes were pre-treated with 10 μM of PDTC before palmitate treatment about 6 h. And then, the cells were treated with 0.5 mM of palmitate for 24 h. Total RNA was extracted from C2C12 myotubes. The RNA (1 μg) was subjected to real-time PCR using primers for SENP2. n=7.

(* = $p < 0.05$)

(A) (B)

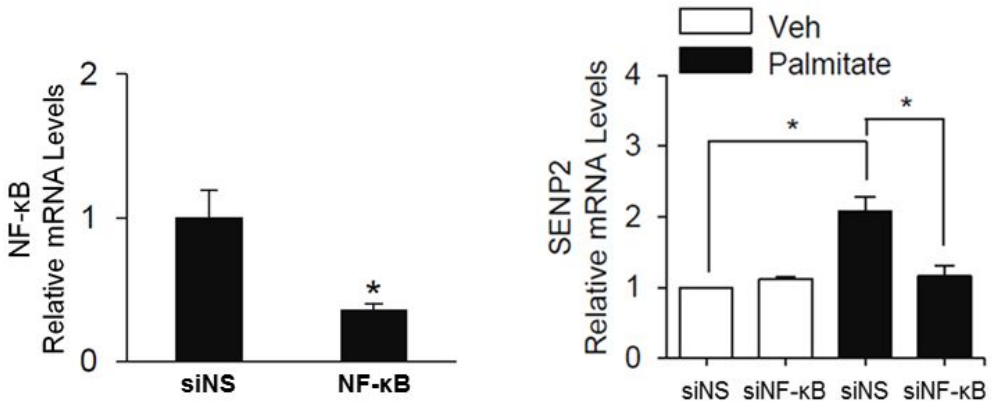

Figure 5. Knockdown of NF-κB inhibits palmitate-induced SENP2 in C2C12 myotubes

C2C12 myotubes were transfected with siRNA (50 ng) of NF-κB for 2 days. And then, the cells were treated with 0.5 mM of palmitate for 24 h. Total RNA was extracted from C2C12 myotubes. (A) The RNA (1 μg) subjected to real-time PCR using primers for NF-κB. Total RNA was extracted from C2C12 myotubes. (* = $p < 0.05$ *vs* siNS) (B) The RNA (1 μg) subjected to real-time PCR using primers for SENP2. n=7. (* = $p < 0.05$)

(A)

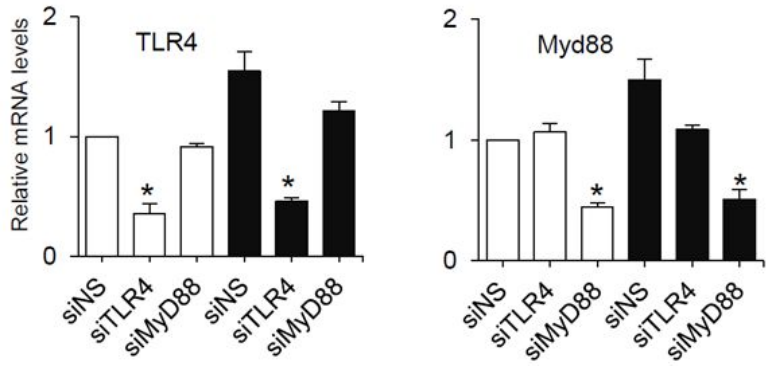
Relative mRNA levels
TLR4
Myd88
2
1
0
*
siNS
siTLR4
siMyD88

(B)

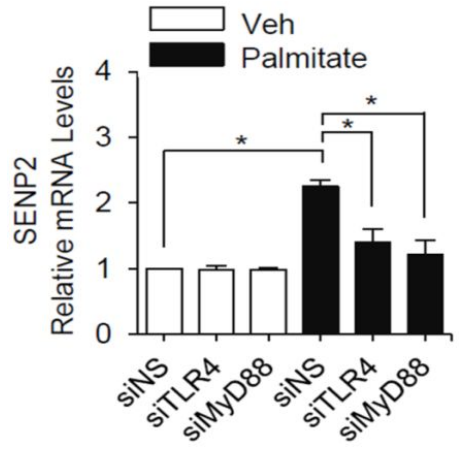
Veh
Palmitate
SENP2
Relative mRNA Levels
4
3
2
1
0
*
siNS
siTLR4
siMyD88

Figure 6. Palmitate increases SENP2 expression via NF-κB activated by TLR4 and Myd88 signaling

C2C12 myotubes were transfected with siRNA (50 ng) of TLR4 or Myd88 for 2 days. And then, the cells were treated with 0.5 mM of palmitate for 24 h. Total RNA was extracted from C2C12 myotubes. (A) The RNA (1 μg) subjected to real-time PCR using primers for TLR4 or Myd88. (* = $p < 0.05$ *vs* siNS) (B) The RNA (1 μg) subjected to real-time PCR using primers for SENP2. n=4. (* = $p < 0.05$ *vs* siNS±palmitate)

(A)

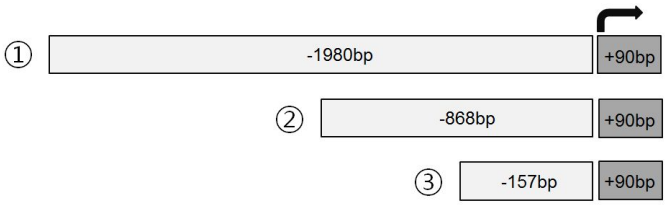
①
-1980bp
+90bp
②
-868bp
+90bp
③
-157bp
+90bp

(B)

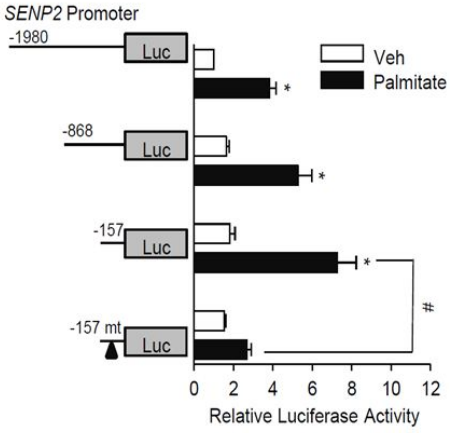
SENP2 Promoter
-1980
Luc
-868
Luc
-157
Luc
-157 mt
Luc
Veh
Palmitate
*
*
*
#
0 2 4 6 8 10 12
Relative Luciferase Activity

(C)

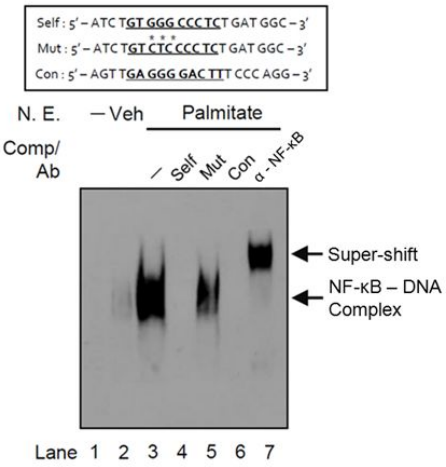
Self : 5′ – ATC TGT GGG CCC TCT GAT GGC – 3′
Mut : 5′ – ATC TGT CTC CCC TCT GAT GGC – 3′
Con : 5′ – AGT TGA GGG GAC TTT CCC AGG – 3′
N. E.
– Veh
Palmitate
Comp/
Ab
–
Self
Mut
Con
α - NF-κB
Super-shift
NF-κB – DNA
Complex
Lane 1 2 3 4 5 6 7

Figure 7. Palmitate increases binding of NF-κB to SENP2 promoter region

C2C12 myoblast were transfected with each construct of SENP2 promoter (0.3 μg/well), pCMV-β-gal (0.1 μg/well) under serum free in DMEM media. And then, the cells were treated with 0.5 mM of palmitate for 24h. Luciferase activity was normalized by β–galactosidasse activity, and the value of the cells transfected with -1980bp construct of SENP2 promoter and treated with vehicle was set to 1 (A). C2C12 myotubes were treated with 0.5 mM of palmitate for 24 h. Nuclear protein were prepared from the C2C12 myotubes, and subjected to EMSA with the labeled probe containing a NF-κB binding site of the SENP2 promoter region. Antibody (10 μg) against NF-κB was used for super-shift (B). n=5. (* = $p < 0.05$)

FAO and expression of FAO-related genes were up-regulated via increase of SENP2 expression by palmitate in C2C12 myotubes

Palmitate treatment led to an increase in the mRNA levels of FAO-associated enzymes, ACSL1, CPT1b and UCP3, in a dose-dependent manner (Figure 8). To confirm whether SENP2 is a mediator in this process, SENP2 was knocked down in C2C12 myotubes (Figure 9A). Knockdown of SENP2 suppressed the increase in palmitate-stimulated FAO level in C2C12 myotubes (Figure 9B). Consistently, increase of FAO related-genes by palmitate were abrogated by SENP2 knockdown (Figure 10). Next, I tested whether palmitate-induced mRNA level increase of FAO-associated enzymes was also mediated by PPARδ and PPARγ recruitment to promoters of CPT1b and ACSL1, and whether SENP2 was involved in the process. The recruitment of PPARδ and PPARγ to the CPT1b or ACSL1 promoters was increased by palmitate and knockdown of SENP2 suppressed the effect of palmitate (Figure 11A, 11B.). These results suggest that SENP2 plays an important role in the palmitate-induced recruitment of PPARδ and PPARγ to the promoters of the FAO-associated enzyme genes.

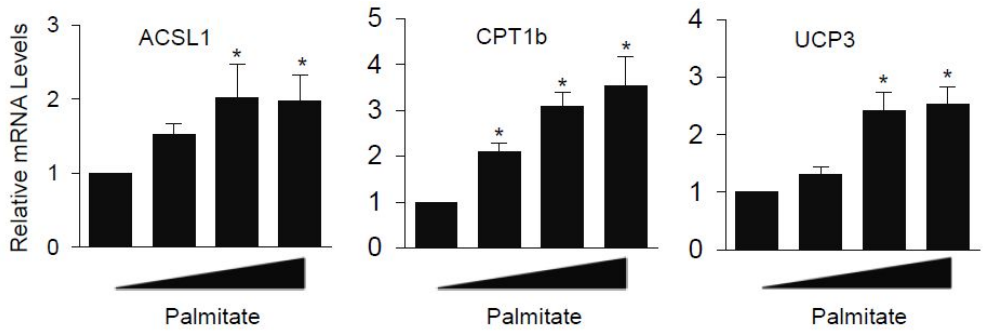

Figure 8. Palmitate up-regulates expression of FAO-related genes in a dose-dependent manner

C2C12 myotubes were treated with 0.25, 0.5 or 1 mM of palmitate for 24 h. Total RNA was extracted from C2C12 myotubes. The RNA (1 μg) was subjected to real-time PCR using primers for SENP2. n=4.

(* = $p < 0.05$ *vs* Veh)

(A) (B)

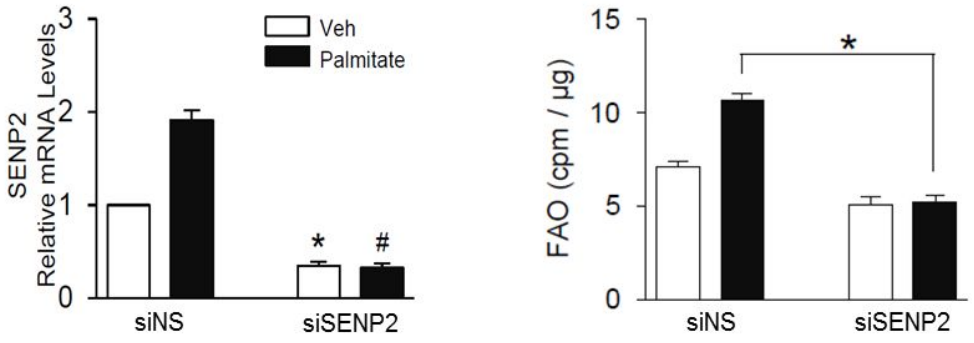

Figure 9. FAO is increased by palmitate via SENP2

C2C12 myotube were transfected with siRNA (50 ng) of SENP2 for 2 days. And then, the cells were treated with 0.5 mM of palmitate for 24 h. Total RNA was extracted from C2C12 myotubes. (A) The RNA (1 μg) subjected to real-time PCR using primers for SENP2. (* = $p < 0.05$ vs siNS + Veh, # = $p < 0.05$ vs siNS + palmitate) (B) Fatty acid oxidation was measured. n=6. (* = $p < 0.05$)

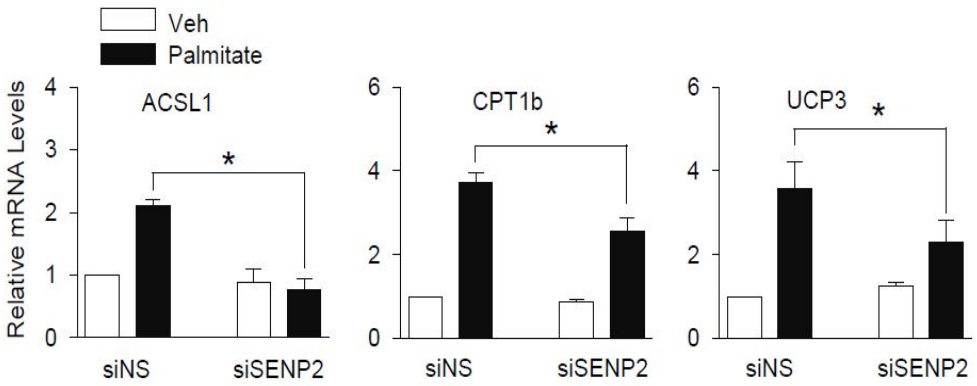

Figure 10. Palmitate-induced increase of mRNA levels of FAO-related genes is mediated bySENP2

C2C12 myotubes were transfected with siRNA (50 ng) of SENP2 for 2 days. And then, the cells were treated with 0.5 mM of palmitate for 24 h. Total RNA was extracted from C2C12 myotubes. The RNA (1 μg) subjected to real-time PCR using primers for ACLS1, CPT1b and UCP3. n=5.

(* = $p < 0.05$)

(A)

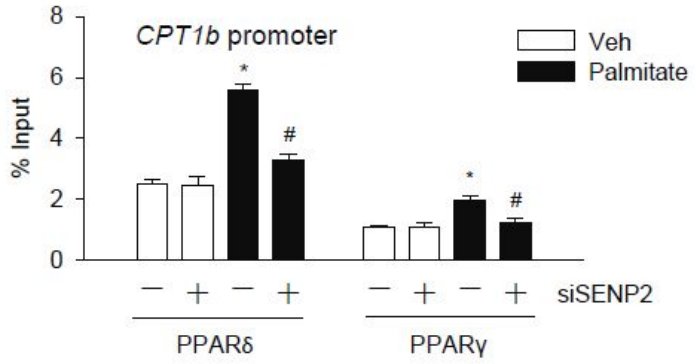

(B)

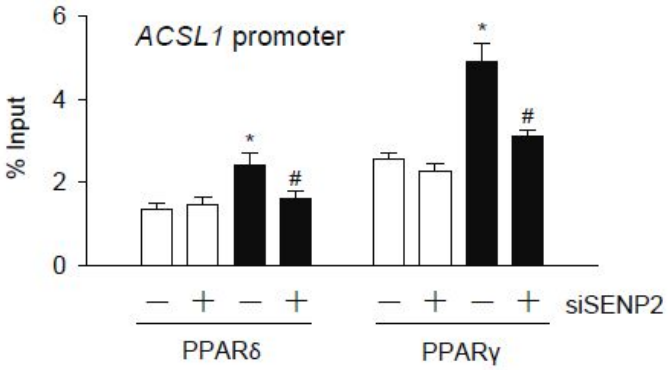

Figure 11. Up-regulation of SENP2 by palmitate leads to binding of PPARδ and PPARγ on promoter regions of CPT1b and ACSL1 genes

C2C12 myotubes were transfected were transfected with siRNA of SENP2 (50 ng/ml) for 2days. And then, the cells were treated with palmitate (0.5 mM) for 24h. ChIP was performed with anti-PPARδ, anti-PPARɣ antibodies (20μg). n=5. (* = $p < 0.05$ *vs* Veh, # = $p < 0.05$ *vs* palmitate)

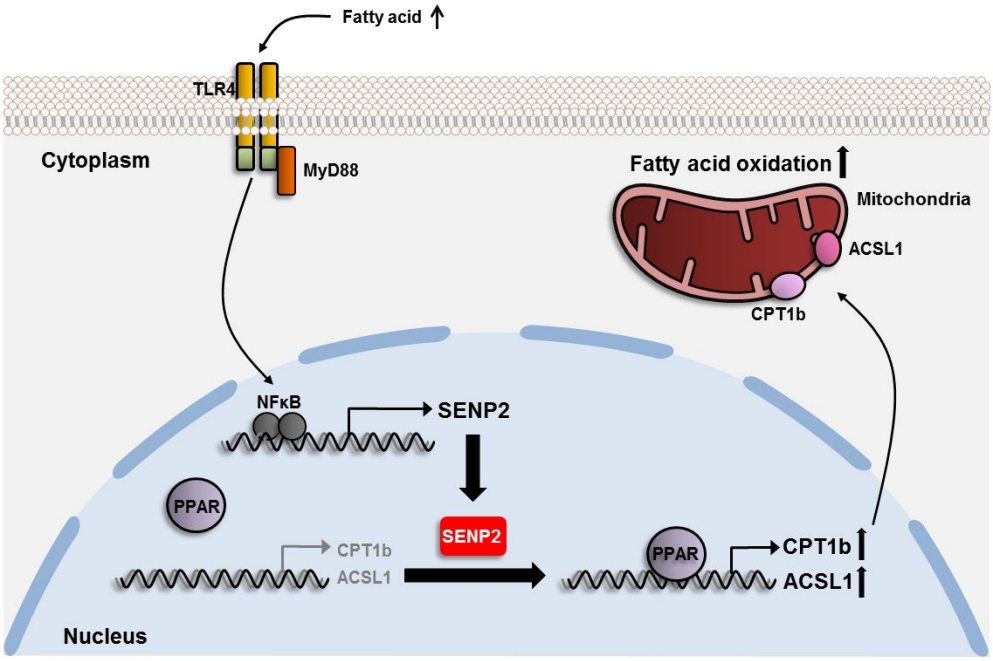

Figure 12. Regulation of SENP2 by fatty acid in the skeletal muscle

DISCUSSION

There are some reports to show the roles of SENP2 in the adipocyte and some cancer cell line. However, any role of SENP2 in the skeletal muscle metabolism has not been revealed. To figure out the metabolic role of SENP2 in skeletal muscle, I started this study from the finding of SENP2 regulator in C2C12 myotubes. SENP2 is up-regulated by saturated fatty acid via TLR4–Myd88–NF-κB signaling pathway (Figure 4-6). Myd88 is a universal adapter protein as it is used by almost all TLRs to activate the transcription factor NF-κB [59]. Typically, TLR4 signaling pathway involved in palmitate-induced cell death and apoptosis by pro-inflammatory signaling [60]. TLR4 activating by palmitate leads to binding NF-κB on the promoter region of SENP2 (Figure 7). However, some papers reported that palmitate induce insulin resistance via TLR2-mediated pro-inflammatory signaling pathway in skeletal muscle or adipocyte [61-64]. So, further study on the role of TLR2 by palmitate is required.

Up-regulated SENP2 by palmitate increase fatty acid oxidation levels and fatty acid oxidation associated genes, such as ACSL1 and CPT1b, in C2C12 myotubes. PPARδ and PPARγ bind to promoter region of ACSL1 and

CPT1b [65, 66]. Also, palmitate induces binding of PPARδ and PPARγ on the promoter region of ACSL1 and CPT1b via SENP2 in C2C12 myotubes. These findings indicate that palmitate could be a source for fatty acid oxidation and regulator of SENP2 in skeletal muscle. Increase of fatty acid oxidation by palmitate can be explained by compensatory mechanism. A paper reported when activation of lipid-derived signals, lipolysis and β-oxidation associated genes are up-regulated in β-cells [67]. However, a question is raised from the results. The question is how to explain increase of mitochondrial dysfunction [68-70], apoptosis [70] and insulin resistance [69] by palmitate. Currently research reported that SENP2 decrease mitochondria mediated neurodegeneration [71] and apoptosis [71, 72]. And deSUMOylation of PGC1α by SENP1 leads to increase of mitochondrial biogenesis [73]. PGC1α is deSUMOylated by SENP2 in C2C12 myotubes, too [54]. Therefore, mitochondrial dysfunction, apoptosis and insulin resistance by palmitate may be improved by palmitate induced SENP2 via compensatory mechanism. These data indicated that palmitate is a important regulator of SENP2.

Saturated fatty acid (palmitate) increase SENP2 expression levels, on the other hand unsaturated fatty acids (oleate, linoleate and EPA) do not increase SENP2 expression levels (Figure 1). Some papers reported different effects

and utilizations of saturated fatty acids and unsaturated fatty acids [74, 75]. ATP levels and ROS productions are impaired by only saturated fatty acid and phosphorylation of JNK by only saturated fatty acid is increased. Above all things, activation of NF-κB by unsaturated fatty acids is not reported. Therefore, compensatory mechanism may be dose not activated by unsaturated fatty acids.

SUMOylation of p53 and ERK5 by SENP2 is important role in endothelial dysfunction and atherosclerosis [76]. Currently research reported that depletion of p90RSK abolishes SUMOylation of p53 and ERK5. And p90RSK-mediated SENP2-T368 phosphorylation decrease p53 SUMOylation and SENP2-T368 phosphorylation by p90RSK causes EC apoptosis and inflammation. p90RSK-SENP2 association is critical for p53 and ERK5 SUMOylation [72]. This paper indicated that localization by phosphorylation of SENP2 is very important endothelial dysfunction and atherosclerosis. Based on this research, it is needed more studies about localization and phosphorylation levels of SENP2 by palmitate in skeletal muscle, adipocyte or β-cells.

Chapter II.

.

Effects of fatty acid metabolism

by SENP2 overexpression

Introduction

Post-translational modifications (PTMs) play important roles in regulating protein stability, trafficking, folding conformation, and functional activity. Small ubiquitin-like modifier (SUMO) protein mediates a type of PTM called SUMOylation in which the SUMO protein is covalently ligated to the target protein through a series of enzymatically-catalyzed reactions and modifies its activities. SUMOylation regulates many cellular processes like transcription, the maintenance of the ion gradient across the cell membrane, stress response, autoimmunity, etc [23, 77]. The SUMO conjugation pathway is similar to that of ubiquitin, but distinct E1 (activating enzyme), E2 (conjugating emzyme), and E3 (ligase) activities are needed for both processes. SUMOs are first activated in an ATP-dependent manner by the dimer of SAE1, 2 and subsequently conjugated by Ubc9. PIAS proteins, nucleoporin RanBP2, and polycomb protein Pc2 are able to enhance SUMOylation in a manner that resembles the action of E3 ligases [23, 77-79]. Several target proteins of SUMOylation are involved in the biological pathways related to various human diseases, including T2DM, obesity, cardiovascular diseases, cancer and neurodegenerative disorders [80-82].

The SUMO modification pathway is a reversible system that is controlled by SUMO-specific protease (SENP) family members. The human genome encodes six dedicated SUMO-specific members of the SENP family: SENP1, SENP2, SENP3, SENP5, SENP6 and SENP7. And they all have a conserved C-terminal catalytic domain and non-conserved N-terminal regions. It is known that SENP2 deSUMOylates Mdm2, an ubiquitin E3 ligase of p53 [83]. The SENP1-SENP2, SENP3-SENP5 and SENP6-SENP7 pairs show the highest degree of similarity to each other. SENP6 and SENP7 are most divergent from the rest of the family and harbor conserved sequence insertions within their catalytic domains [84-86]. However, it is little known about the role of SENPs in the regulation of energy metabolism.

Recent studies have shown that SENP2 represses glycolysis and reprograms glucose metabolism in cancer cells and SENP1 overexpression increases mitochondrial biogenesis in myotubes [73]. Overexpression of SUMO1 in mammalian cancer cells resulted in increased hypoxia-induced glycolysis and resistance to hypoxia-dependent ATP depletion. Conversely, cells overexpressing the SENP2 failed to demonstrate hypoxia-induced glycolysis [87]. IFNγ, or type II interferon, is a cytokine that is critical for innate and adaptive immunity against bacterial infections. IFNγ is an important activator of macrophages and inducer of Class II major

histocompatibility complex (MHC) molecule expression. IRF3 is a member of the interferon regulatory transcription factor (IRF) family. SENP2 is a negative regulator of IFNγ and regulates the stability by IRF3 deSUMOylation. Also, SENP2 overexpression leads to ubiquitination of IRF3. These findings suggest that SENP2 regulates antiviral innate immunity by deSUMOylating IRF3 and controls ubiquitination and degradation in cross-talk between ubiquitin and SUMO [88].

Recently, genetically modified mouse, such as transgenic and knockout mouse, is commonly used for research or as animal models of human diseases. Mouse is a useful model for genetic research, as their tissues and organs are similar to that of a human [89]. Research using skeletal muscle specific transgenic mouse started from muscle cell differentiation and growth studies. The mouse is genetically engineered for increase of muscle growth and strength by overexpression of insulin-like growth factor I (IGF-I) in differentiated muscle fibers [90, 91]. About 3 decades ago, energy metabolism associated research started using muscle and liver specific transgenic mouse [92, 93]. Experiments using a transgenic mouse expressing creatine kinase in liver to understand ATP catabolism and regulation of oxidative phosphorylation are discussed [92]. Also, research on energy balance and lipid metabolism in transgenic mice was started [94]. Many

research reported various results using SENPs transgenic or knockout mouse in various fields. SENP1 transgenic mice showed increase of HIF1α expression with progression of the dysplasia. The enhanced HIF1α stability in the SENP1 transgenic mice produced elevated VEGF expression. Consequently, it is not surprising that angiogenesis was readily observed in these SENP1 transgenic mice compared with age-matched wild-type mice [95]. In SENP1 or SENP2 knockout mice, both proteases are essential to embryo viability, suggesting that the SUMO pathway components played an essential role in normal murine embryogenesis [80, 81]. Furthermore, elevated levels of SENP1 have been observed in thyroid adenocarcinoma and prostate cancer [96, 97]. SENP2 is essential to trophoblast development, through modulation of the p53/mouse double minute-2 pathway [81]. Knockout mouse models have also evidenced a crucial role for SENP2 in regulating adipogenesis by targeting CCAAT/enhancer-binding protein-β [53], whereas SENP2 overexpressing induce severe cardiac dysfunction [98]. SENPs, including SENP2, are reported to modulate the activity of transcription factors, such as androgen receptor (AR) [99] and progesterone receptor (PR) [100].

As mentioned above, I hypothesized that SENP2 is involved in energy and lipid metabolism in skeletal muscle. Further to chapter I, I investigated that

metabolic effects by SENP2 overexpression in C2C12 myotubes and skeletal muscle specific transgenic mouse models.

Material and Method

Microarray

Gene expression of C2C12 cells were profiled using MouseRef-8-v2-BeadChip (Illumina, CA, USA). The array was scanned using a BeadStation 500 System (Illumina, CA, USA).

Plasmid and adenovirus

SENP1 expression vectors and FLAG-tagged SUMO1, SENP2 expression vectors were generously provided by Dr C. H. Chung (School of Biological Sciences, Seoul National University, Seoul, Korea). SENP2 mutants, C548S, were generated by site-directed mutagenesis (Stratagene, Agilent Technologies, CA, USA). pPPRE-pk-Luc was generously provided by Dr S. H. Koo (Department of Biological Sciences, Korea University). An expression vector for PGC1α was obtained from Dr. Gang Xu (CUHK, Hong Kong). Adenovirus containing the human SENP1, SENP2, SENP2mt were prepared from the expression vectors of each genes.

Cell culture

C2C12 myoblasts were maintained in DMEM supplemented with 10% FBS (Invitrogen, MA, USA). Differentiation was induced using DMEM containing 2% horse serum (Invitrogen, MA, USA) for 4 days. Transfection of plasmids was performed using Lipofectamin with Plus Reagent (Invitrogen, MA, USA), and siRNAs were transfected using RNAiMAX (Invitrogen, MA, USA) for 3 days before cell harvest. Adenovirus of each gene was transfected for 3 days before cell harvest. COS7 cells were maintained in DMEM supplemented with 10% FBS (Invitrogen, MA, USA).

siRNA treatment

Small interfering RNAs (siRNAs) of PPARs, PGC1α, ERRα and RIP140 were purchased from Dhamacon (Chicago, IL, USA) and nonspecific siRNAs (negative control) were purchased from BIONEER (Daejeon, Korea). 50 nM of siRNA or siNS was mixed with RNAiMAX (Invitrogen, MA, USA) in 100 μl of serum-free DMEM and incubated for 30 min at room temperature. The complex was treated to the cells with 400 μl of serum-free DMEM. After 4 hour incubation, 500 μl of DMEM media supplemented with 2% horse serum were added.

RNA preparation and Real-time PCR

Total RNAs of differentiated C2C12 cells were isolated using TRIzol (Invitrogen, MA, USA) according to the manufacturer's instruction. To prepare cDNA, 10 μl of reaction buffer (Invitrogen, MA, USA), 5 μl of 100 mM DTT, 2.5 μl of 10 mM dNTP, 1 μl of Oilgo dT, 0.5 μl of RNase inhibitor, 2 μl of RTase and 1 ug of RNA were mixed and RNase free water was added up to 50 μl. The mixture was incubated at 37 for 1 hour and at 72°c for 10 min using PCR system. Expression levels of genes were determined by using SYBR-MASTER MIX (Takara, Otsu, Shiga, Japan) and ABI 7500 Real-time PCR system (Applied Biosystem, CA, USA).

Western Blotting

Tissues and cells were lysed in 20 mM Tris-HCl, pH 7.4, 1 0mM $Na_4P_2O_7$, 100 mM NaF, 2 mM Na_3VO_4, 1% NP-40 buffer supplemented with protease inhibitor (10 μg/μl aprotinin, 10 μg/μl luepeptin and 1mM PMSF). The whole-cell lysates were sonicated 15 seconds for two times, and cell debris was removed by centrifugation (13,000 rpm) for 30 min at 4°c. About 20~30 μg of proteins were separated on the SDS-PAGE. Separated proteins were transferred onto nitrocellulose membrane (Whatman, Dassel, Germany). The membrane was blocked with 5% skim milk in Tween020-Tris-buffered

saline (TBS-T) for 1~2 h at room temperature, and it was incubated with the specific primary antibody for overnight at 4°c. Membranes were probed with specific antibodies and bands were visualized by enhanced chemi-luminescence (Pierce, IL, USA).

Measurement of Fatty Acid Oxidation

For measurement of FAO, muscle tissues or cells were homogenized in an ice-cold mitochondria isolation buffer (250 mmol sucrose, 10 mmol Tris-HCl, and 1 mmol EDTA). The lysates were incubated for 2 h with 0.2 mmol [1-^{14}C]palmitate. $^{14}CO_2$ and ^{14}C-labeled acid-soluble metabolites were quantified using a liquid scintillation counter. Each radioactivity was normalized by protein amount of each lysate.

Immunoprecipitation

Tissues and cells were prepared with the lysis buffer (20 mM Tris-HCl pH 7.4, 1% Triton X-100, 1% Sodium deoxycholate, 0.1% SDS, 150 mM NaCl, 1 mM EGTA, 10 mM $Na_4P_2O_7$, 100 mM NaF, 2 mM Na_3VO_4, 10 μg/μl aprotinin, 10 μg/μl luepeptin and 1mM PMSF) (Sigma, St. Louis, MI, USA) for Immunoprecipitation assay. Cell debris was removed by centrifugation

for 30 min at 4°c. Protein concentration was determined by Bradford assay (Bio-Rad, Hercules, CA, USA). Lysate (700 µg) were incubated with anti-HA (12CA5) (Roche, Mannheim, Germany) and Protein G Separose (GE Healthcare, Uppsala, Sweden) for overnight at 4°c. The beads were washed twice with the lysis buffer and phosphate-berffered saline (PBS), respectively. The IP samples were eluted in Laemmli sample buffer (62.5 mM Tris-HCl pH 6.8, 2% SDS, 25% glycerol, 5% 2-mercaptoethanol, 0.01% Bromophenol Blue) (Sigma, St. Louis, MI, USA).

ChIP (Chromatin Immunoprecipitation)

C2C12 myotubes were transfected 50moi of Ad-GFP, Ad-SENP2 and Ad-SENP2mt for 3 days before harvest. Also, C2C12 myotubes were transfected with siRNA (50 nM) of SENP2 for 3 days and treated with palmitate (0.5 mM) for 24 h before harvest. After cross-linking and DNA fragmentation, nuclear extracts were immunoprecipitated with PPARα, PPARδ, PPARɣ and PGC1α antibodies or control IgG. Primers used for real-time PCR were 5'-GAG CAG CAG TGG TCC CTG AG-3' and 5'-TGC TGG AAG GTC TGG GAC TG-3' for CPT1b-PPRE ; 5'-GGT GAC TCT ACT CTC AGC TGC-3' 5'-CTTACCAGGCTGCCAAGGTCT -3' for ACSL1-PPRE.

Animals and Metabolic analysis

All aspects of animal care and experimentation were conducted in accordance with the National Institutes of Health "Guide for the Care and Use of Laboratory Animals" (NIH Publication No. 85-23, revised 1996). The mice were genotyped after 3 weeks from birth and were fed HFD after 3 weeks from genotyping. HFD (60% high fat and high sucrose) period was for 12 weeks. The mice were dual-energy X-ray absorptiometry (DXA) scanned using LUNAR Prodigy scanner with software version 8.10 (GE Healthcare, PA, USA) before sacrifice. The levels of free fatty acid and triglyceride were measured by BioVision kit (BioVision, CA, USA). For electron microscopical analysis, thin muscle sections were prepared and examined using a transmission electron microscope (JEM-1400,JEOL, MA, USA) at 80 Kv. Insulin levels of serum (5 μl) were measured by ALPICO Ultrasensitive kit (ALPCO, NA, USA). Glucose (1 g/kg) tolerance test and insulin (1 unit/kg) resistance test were performed after HFD 12 weeks.

ATP bioluminescent somatic cell assay

Tissues and cells were lysed in somatic cell ATP releasing reagent (Sigma Aldrich, St. Louis, MO, USA), to increase membrane permeability and to release cellular ATP. Then these cellular ATPs were reacted with ATP assay

mix (Sigma Aldrich, St. Louis, MO, USA), containing luciferase, luciferin, $MgSO_4$, DTT, EDTA, bovine serum albumin and tricine buffer salts. The relative amount of ATP released was determined by the light emitted from above reaction.

Statistical analysis

Statistical analysis was performed using SPSS version 12.0 (SPSS Inc.). Statistical significance was tested using the Mann-Whitney U test. A *P* value below 0.05 was considered statistically significant.

Results

Microarray analysis for the effects of SENP2 overexpression in C2C12 myotubes

C2C12 myotubes were infected with adeno viruses having SENP2 overexpression system (50 moi) for 3 days, and then total RNA was isolated from the C2C12 myotubes. Total RNA samples were prepared as a triplet for microarray analysis. When SENP2 was overexpressed in C2C12 myotubes, mRNA levels of the genes related with glucose metabolic process, fatty acid metabolism, muscle cell differentiation, calcium ion transport and glucose transport related genes were up-regulated versus control (Figure 13A). On the other hand, mRNA levels of the genes related with cell cycle, DNA replication, chromosome organization, cytoskeleton organization, RNA processing and ribosome biogenesis were down-regulated versus control (Figure 13A). In addition, SENP2 increased expression of phosphorylation-related genes, such as COX and NDUF family. COX and NDUF family proteins are crucial component factors of mitochondria complex subunits and have very important roles in the mitochondria respiration. Furthermore,

SENP2 increased fatty acid metabolism-related genes, including ACSL1 and CPT1b. ACSL1 and CPT1b play very important roles in fatty acid oxidation (Figure 13B). Figure 13 is contributed by pf. DeaHee Hwang in DIGIST.

(A)

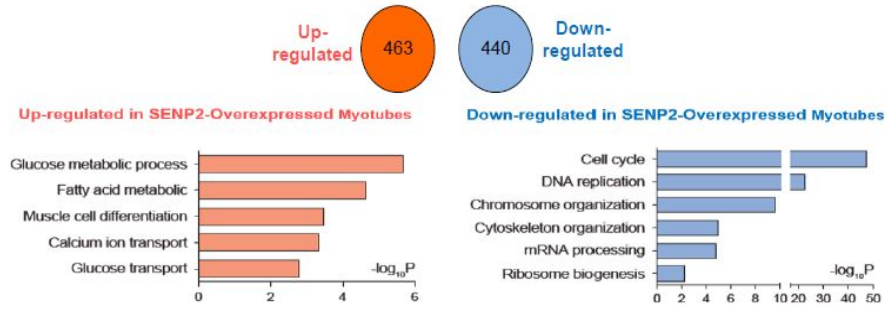
Up-regulated
463
440
Down-regulated
Up-regulated in SENP2-Overexpressed Myotubes
Glucose metabolic process
Fatty acid metabolic
Muscle cell differentiation
Calcium ion transport
Glucose transport
-log10P
0
2
4
6
Down-regulated in SENP2-Overexpressed Myotubes
Cell cycle
DNA replication
Chromosome organization
Cytoskeleton organization
mRNA processing
Ribosome biogenesis
-log10P
0
2
4
6
8
10
20
30
40
50

(B)

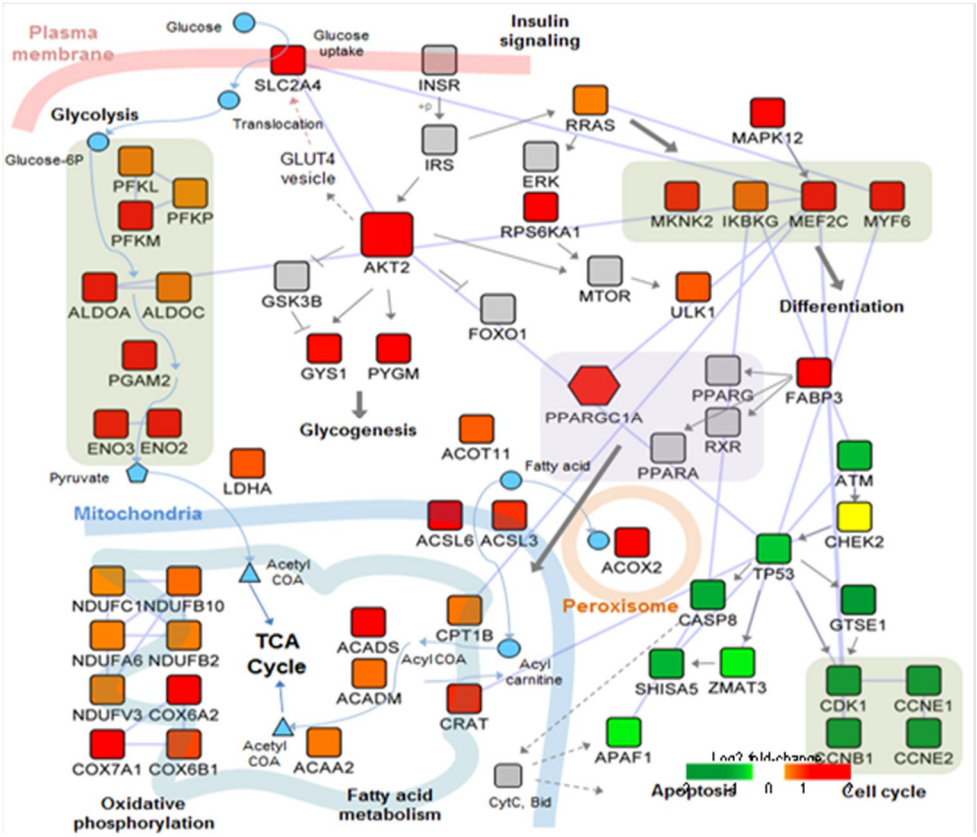
Plasma membrane
Glucose
Glucose uptake
SLC2A4
Translocation
GLUT4 vesicle
Insulin signaling
INSR
IRS
RRAS
MAPK12
ERK
RPS6KA1
MKNK2
IKBKG
MEF2C
MYF6
Differentiation
AKT2
GSK3B
MTOR
ULK1
FOXO1
Glycolysis
Glucose-6P
PFKL
PFKP
PFKM
ALDOA
ALDOC
PGAM2
ENO3
ENO2
Pyruvate
LDHA
GYS1
PYGM
Glycogenesis
PPARGC1A
PPARG
FABP3
RXR
PPARA
ACOT11
Fatty acid
ATM
CHEK2
TP53
Mitochondria
ACSL6
ACSL3
ACOX2
Peroxisome
CASP8
GTSE1
SHISA5
ZMAT3
CDK1
CCNE1
CCNB1
CCNE2
Acetyl COA
NDUFC1
NDUFB10
NDUFA6
NDUFB2
NDUFV3
COX6A2
COX7A1
COX6B1
TCA Cycle
ACADS
ACADM
ACAA2
CPT1B
AcylCOA
Acyl carnitine
CRAT
APAF1
CytC, Bid
Apoptosis
Cell cycle
Oxidative phosphorylation
Fatty acid metabolism

Figure 13. Microarray analysis

C2C12 myotubes were infected with SENP2 adeno virus (50 moi) for 3 days. Total RNA was isolated from the C2C12 myotubes. Total RNA samples were prepared for microarray analysis. (A) Wide cell signaling pathway and (B) mitochondrial signaling pathway of the RNA samples were analyzed.

Overexpression of SENP2 increases FAO primarily by up-regulating the expression of FAO-associated enzymes

To confirm the results of microarray and animal studies, C2C12 myotubes were infected with adenovirus overexpressing SENP1, SENP2, and its catalytically inactive form (C548S) (referred to as Ad-SENP1, Ad-SENP2, and Ad-SENP2mt, respectively) (Figure 14A). Consistent with the data from microarray analysis and animal studies, overexpression of SENP2, but not SENP1 or SENP2mt, led to an increase FAO levels (Figure 14B). Generally, long-chain acyl-CoA synthase 1 (ACSL1) and carnitine-palmitoyl transferase-1(CPT1) are known to play a critical role in fatty acid oxidation (FAO) [101, 102]. The increase in FAO-related genes, *ACSL1*, *CPT1b* and *UCP3* by overexpression of SENP2 was significantly higher than that by overexpression of SENP1 or SENP2mt (Figure 14C). On the other hand, overexpression of SENP2 showed no big difference on the expression of mRNAs for transcription factors involved in lipid metabolism, such as PPARα, PPARδ, PPARγ, PGC1α, and estrogen-related receptor α (ERRα) (Figure 15). These results suggest that the deSUMOylating activity of SENP2 is required for the promotion of FAO via up-regulation of the expression of FAO-associated enzymes in C2C12 myotubes.

(A)

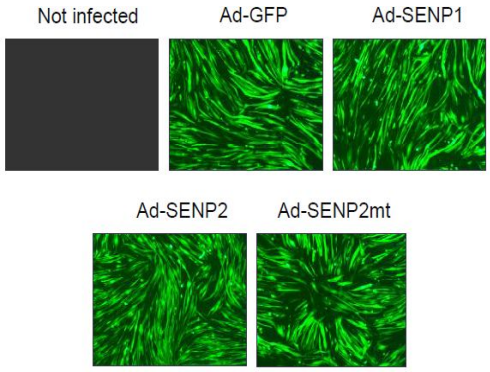
Not infected
Ad-GFP
Ad-SENP1
Ad-SENP2
Ad-SENP2mt

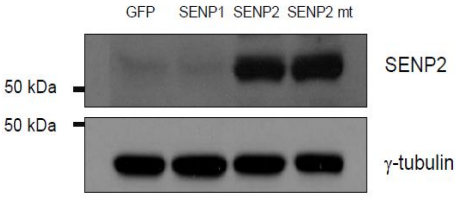
GFP
SENP1
SENP2
SENP2 mt
50 kDa
50 kDa
SENP2
γ-tubulin

(B)

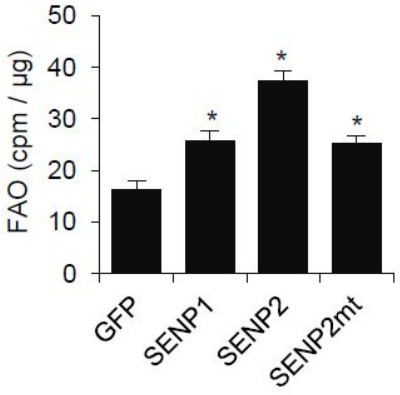
FAO (cpm / μg)
50
40
30
20
10
0
*
*
*
GFP
SENP1
SENP2
SENP2mt

(C)

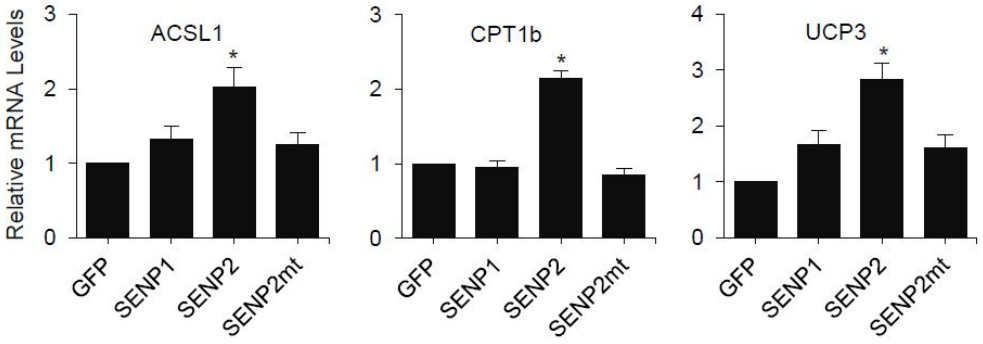
Relative mRNA Levels
ACSL1
CPT1b
UCP3
GFP
SENP1
SENP2
SENP2mt

Figure 14. SENP2 increases FAO and expression of FAO-related genes in C2C12 myotubes

(A) C2C12 myoblast were differentiated under 2% horse serum in DMEM media. After 3 days, C2C12 myotubes were infected with SENP1, SENP2 and SENP2mt adeno-virus (50 moi) for additional 3 days. (B) Fatty acid oxidation was addition of C^{14}-palmitate in the reaction buffer for 2 h. (C) Total RNA was extracted from C2C12 myotubes. The RNA (1 μg) subjected to real-time PCR using primers for fatty acid oxidation related genes. (n=5)

(* = $p < 0.05$ *vs* Ad-GFP)

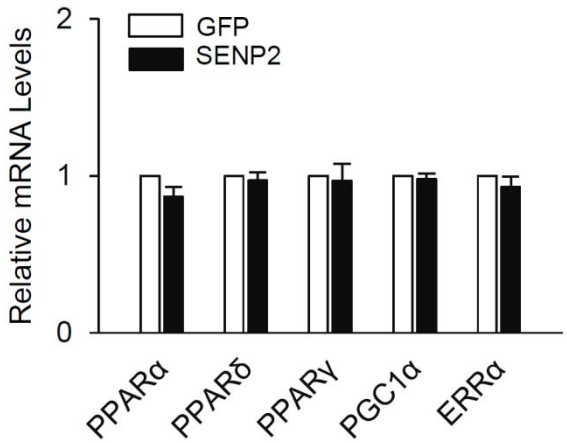

Figure 15. Expression levels of transcription factors by SENP2 overexpression

C2C12 myotube were transfected with GFP and SENP2 adeno-virus (50 moi) for 3 days. Total RNA was extracted from C2C12 myotubes. The RNA (1 μg) subjected to real-time PCR using primers for transcription factors. (n=5)

SENP2 increases FAO mainly by promoting PPARδ and PPARγ mediated expression of FAO-associated enzymes

To determine whether SENP2-dependent increase in the expression of FAO-associated enzymes is mediated by deSUMOylation of transcription factors that are involved in lipid metabolism, I first performed knockdown analysis to each of them. Each siRNA used effectively knocked down the mRNA of transcription factors, PPARα, PPARδ, PPARγ, PGC1α, ERRα, and RIP140 (Figure 16A). Interestingly, knockdown of PPARδ and PPARγ dramatically suppressed SENP2-mediated increase of the FAO levels (Figure 16B). Also, knockdown of PPARδ and PPARγ dramatically suppressed SENP2-mediated increase in the mRNA levels of FAO-associated enzymes (Figure 16C). On the other hand, the basal FAO level was not affected by knock down of any of the transcription factors, including PPARδ and PPARγ (Figure 17). These results suggest that SENP2 increases FAO mainly by promoting PPARδ and PPARγ mediated expression of FAO-associated enzymes. To determine whether SENP2 influences the recruitment of PPARδ and PPARγ to the promoters of their target genes such as *ACSL1* and *CPT1b*, chromatin immunoprecipitation coupled quantitative real time PCR analysis (ChIP-qPCR) was performed using C2C12 myotubes that had been

transfected with Ad-GFP, Ad-SENP2, and Ad-SENPmt. Overexpression of SENP2 markedly promoted the binding of PPARδ and PPARγ to the promoter region of CPT1b (Figure 18A). Similar results were obtained using the *ACSL1* promoter region (Figure 18B). However, binding of PPARα or PGC1α was not affected by SENP2 overexpression (Figure 18A, 18B). These results indicate that SENP2 increases mRNA expression of FAO-associated enzymes by promoting the recruitment of PPARδ and PPARγ to the promoters of the genes.

(A)

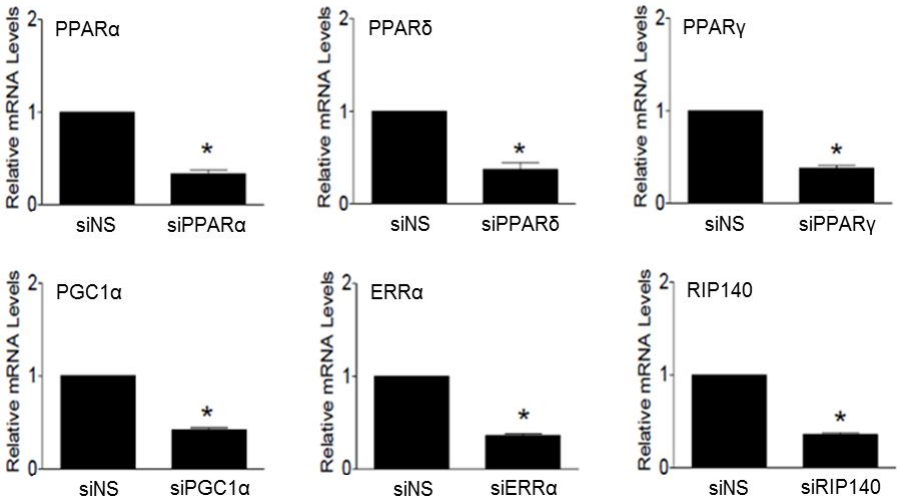
PPARα
PPARδ
PPARγ
PGC1α
ERRα
RIP140
Relative mRNA Levels
siNS
siPPARα
siPPARδ
siPPARγ
siPGC1α
siERRα
siRIP140

(B)

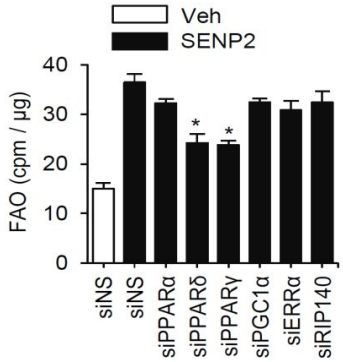
Veh
SENP2
FAO (cpm / μg)
siNS
siPPARα
siPPARδ
siPPARγ
siPGC1α
siERRα
siRIP140

(C)

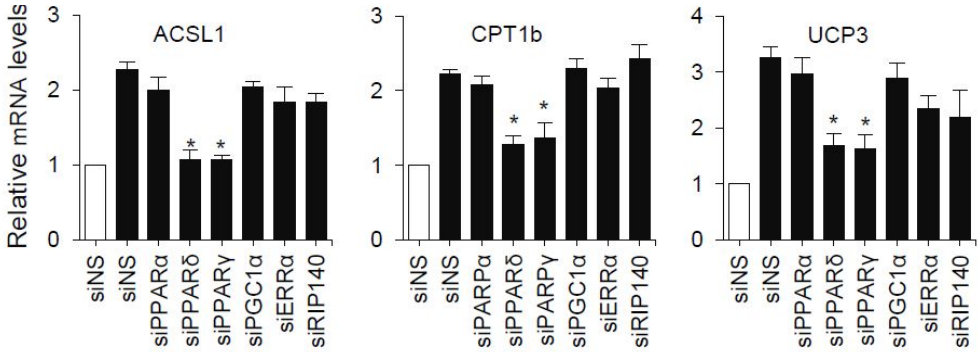
ACSL1
CPT1b
UCP3
Relative mRNA levels
siNS
siPPARα
siPPARδ
siPPARγ
siPGC1α
siERRα
siRIP140

Figure 16. FAO and mRNA levels of FAO-related genes are increased by SENP2 via PPARδ and PPARγ

C2C12 myoblast were differentiated under 2% horse serum in DMEM media. After 3 days, C2C12 myotubes were transfected with siRNA (50 ng) of each transcription factor. After C2C12 myotubes were infected with transfected Ad-GFP or Ad-SENP2 (50 moi) for 3days. (A) The RNA (1 μg) subjected to real-time PCR using primers for transcription factor genes. (B) Fatty acid oxidation was measured. Total RNA was extracted from C2C12 myotubes. (C) The RNA (1 μg) subjected to real-time PCR using primers for fatty acid oxidation related genes. n=5. (* = $p < 0.05$ *vs* siNS + Ad-SENP2)

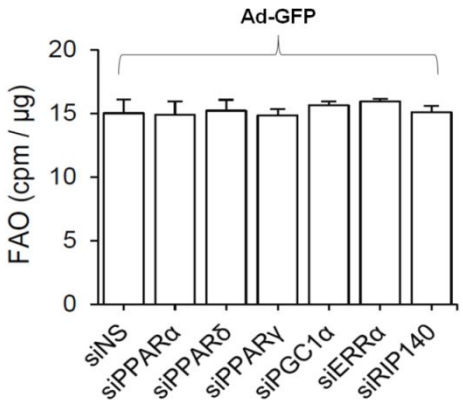

Figure 17. Knock-down of transcription factors does not change the basal FAO levels

C2C12 myoblast were differentiated under 2% horse serum in DMEM media. After 3 days, C2C12 myotubes were transfected with siRNA (50 ng) of each transcription factor. After C2C12 myotubes were infected with Ad-GFP (50 moi) for 3 days.

(A)

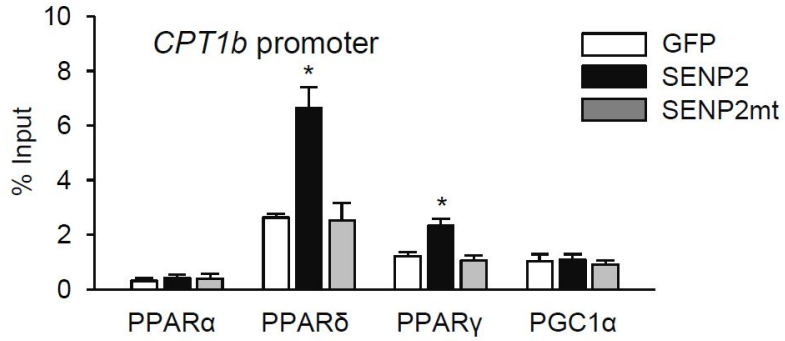

(B)

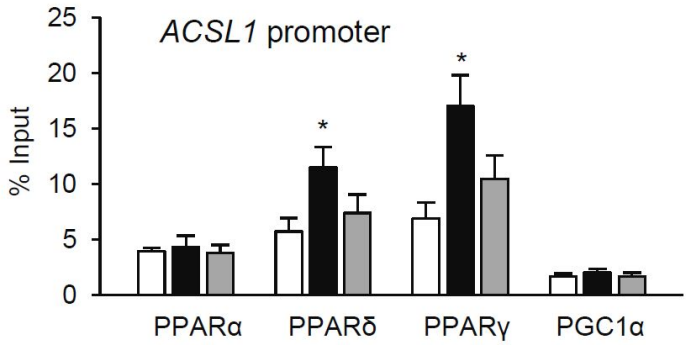

Figure 18. Binding of PPARδ and PPARγ to the promoter regions of the FAO-related genes is increased by SENP2

C2C12 myotubes were transfected were infected with Ad-GFP, Ad-SENP2 and Ad-SENP2mt (50 moi) for 3 days. ChIP was performed with anti-PPARα, anti-PPARδ, anti-PPARγ or anti-PGC1α antibodies (20 μg). Real-time PCR was performed with the PPRE sites on the promoter regions of (A) *CPT1b* and (B) *ACSL1*. For input, 1/10 volume of sample for immunoprecipitation was used for real-time PCR. n=4. (* = $p < 0.05$ *vs* Ad-GFP)

SENP2 promotes PPARδ activity by deSUMOylation

Our laboratory have previously shown that SENP2 deSUMOylates PPARγ and promotes its activity [53]. In general, PGC1α and KLF5 were known to deSUMOylate by SENP2 or SENP1 [44, 54, 73]. However, it is not clear about SUMOylation of PPARδ. To determine whether PPARδ also is a target for SENP2, I first examined whether PPARδ is SUMOylated. Sequence analysis revealed that PPARδ contains the MK104LE sequence which is similar to the consensus SUMOylation ΨKXE motif, where Ψ is a hydrophobic amino acid and X is any amino acid (Table 2). Therefore, I replaced the Lys104 residue by Arg to test if the mutation (K104R) influences PPARδ SUMOylation. Overexpression of SUMO1 and UBC9 (SUMOylation E2 enzyme) with PPARδ, but not with its K104R mutant, dramatically increased the appearance of slow-migrating PPARδ bands (Figure 19). Furthermore, the slow-migrating bands could completely be eliminated by the expression of SENP2, but not by SENP2mt (Figure 20). These results indicate that PPARδ, like PPARγ, serves as a target of SENP2 and its Lys104 residue is a major SUMO acceptor site. The higher molecular weight bands were also detected with anti-ubiquitin antibody as well as anti-SUMO antibody, and ubiquitination of PPARδ was increased when

SUMOylation was accompanied (Figure 21). Figure 19-21 are contributed by pf. JeaHong Seol in Seoul National University.

Therefore, it is possible that SUMOylation of PPARδ promotes ubiquitination, which generates multiple high molecular weight bands. Also, I confirmed deSUMOylation of endogenous PPARδ by SENP2 overexpression in myotubes (Figure 22). To examine whether PPARδ SUMOylation affects its activity, COS7 cells were transfected with a PPRE-TK-Luc reporter vector. In generally, PGC1α is essential factor for role performance of PPAR family [103-105]. Because the levels of PGC1α expression is very low in COS7 cells, co-expression of PGC1α was necessary to detect the PPARδ activity in non-muscle COS7 cells, which were used instead of C2C12 myotubes having very low transfection efficiency. Overexpression of SENP2 dramatically increased the activity of PPARδ. Remarkably, the activity of SUMOylation-deficient K104R seen without SENP2 was nearly as high as that of wild-type PPARδ seen with SENP2, indicating that SENP2-mediated deSUMOylation is required for PPARδ to show its maximal activity (Figure 23). Taken together, these results indicate that SENP2 promotes the activity of PPARδ as well as PPARγ through deSUMOylation.

	SUMOylation site
PPARγ	IK(107)VE
PPARδ	**MK(104)LE**
PGC1α	VK(183)TE
KLF5	IK(162)TE & IK(209)QE

Table 2. PPARδ has a SUMOylation site

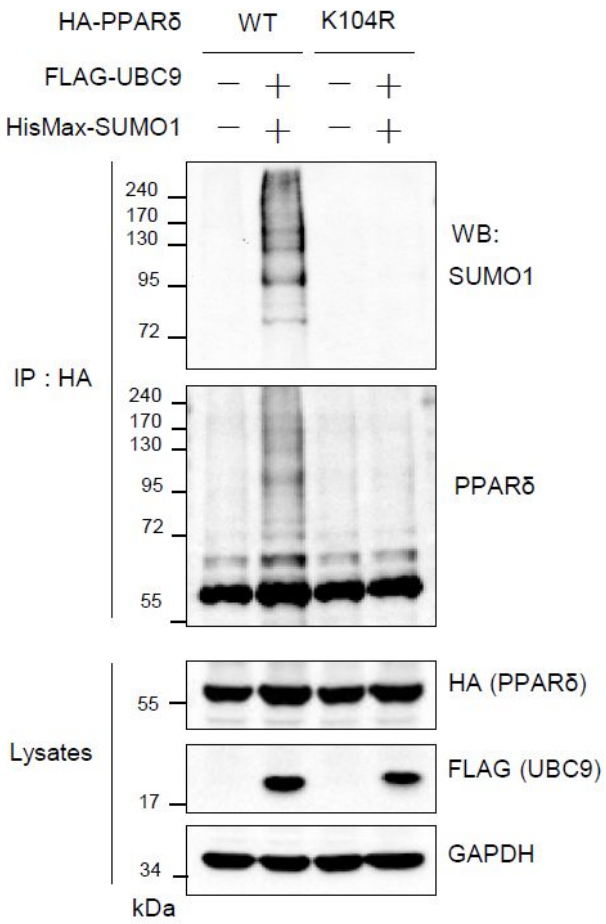

Figure 19. PPARδ is deSUMOylated by SUMO1

COS7 cells were transfected with expression vectors of HA-PPARδ, HA-PPARδK104R, HisMax-SUMO1 and flag-UBC9. Cell lysates were subjected to immunoprecipitation with anti-HA antibody followed by immunoblot with anti-SUMO1 and anti-PPARδ. The lysate were subjected to immunoblot with anti-HA, anti-flag and anti-GAPDH.

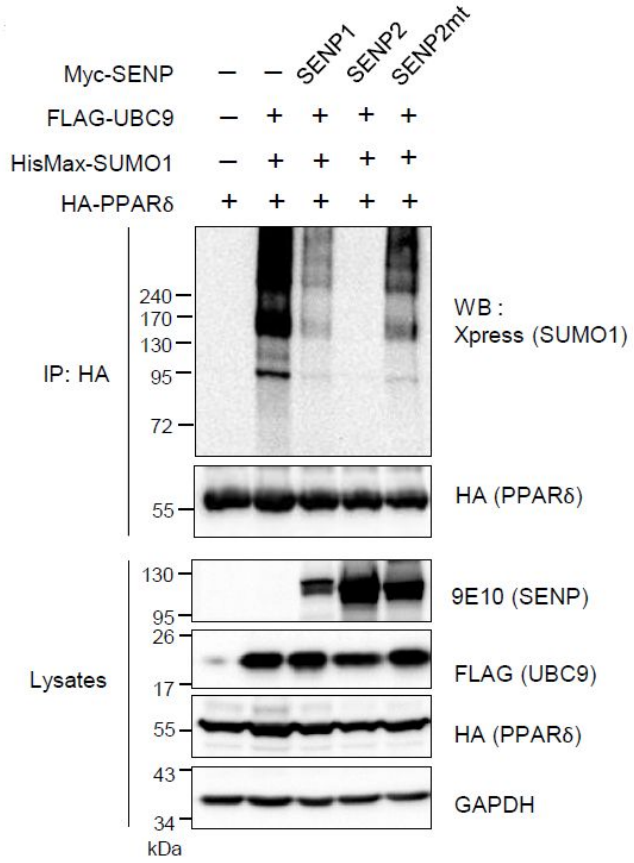

Figure 20. PPARδ is deSUMOylated by SENP2

COS7 cells were transfected with expression vectors of HA-PPARδ, HA-PPARδK104R, HisMax-SUMO1, flag-UBC9, myc-SENP1, myc-SENP2 and myc-SENP2mt. Cell lysates were subjected to immunoprecipitation with anti-HA antibody followed by immunoblot with anti-SUMO1 and anti-PPARδ. The lysate were subjected to immunoblot with anti-SENP, anti-HA, anti-flag and anti-GAPDH.

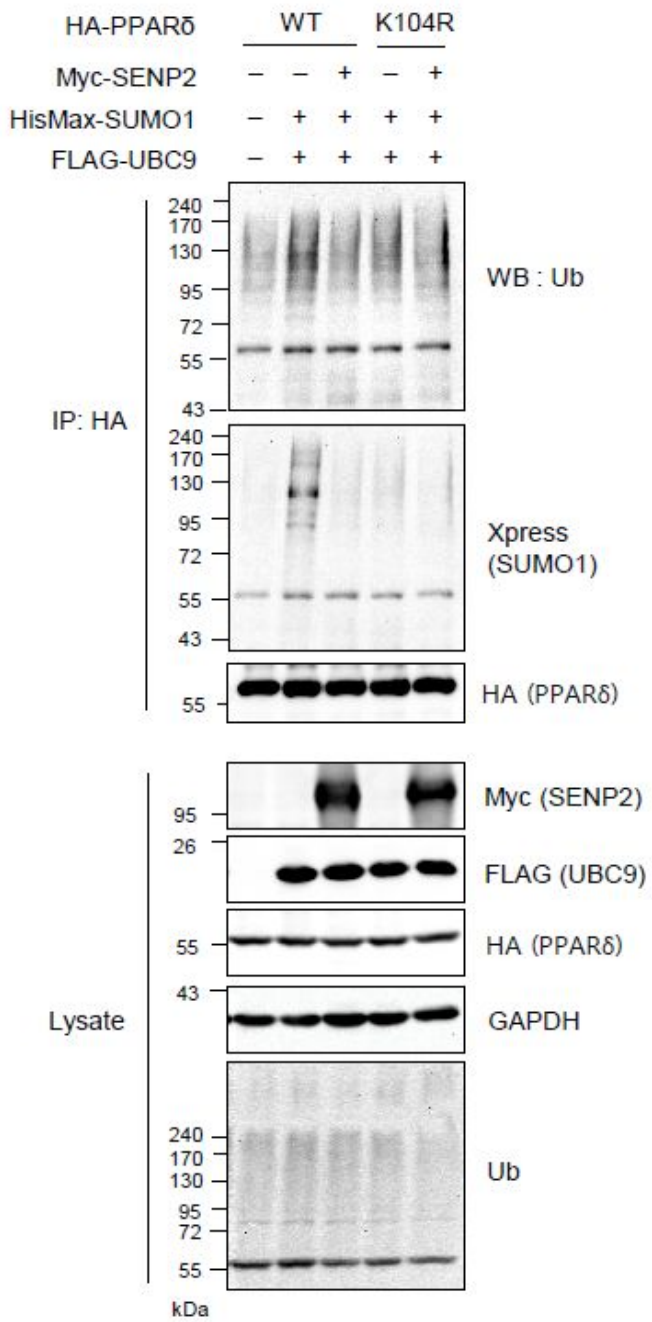
HA-PPARδ
WT
K104R
Myc-SENP2
HisMax-SUMO1
FLAG-UBC9
IP: HA
WB : Ub
Xpress (SUMO1)
HA (PPARδ)
Lysate
Myc (SENP2)
FLAG (UBC9)
HA (PPARδ)
GAPDH
Ub
kDa

Figure 21. SUMOylation of PPARδ may promotes ubiquitination

COS7 cells were transfected with expression vectors of HA-PPARδ, HA-PPARδK104R, HisMax-SUMO1, flag-UBC9, myc-SENP1, myc-SENP2 and myc-SENP2mt under serum free in DMEM media. Cell lysates were subjected to immunoprecipitation with anti-HA antibody followed by immunoblot with anti-Ubiquitin and anti-PPARδ. The lysate were subjected to immunoblot with anti-myc, anti-HA, anti-flag, anti-GAPDH and anti-Ubiquitin.

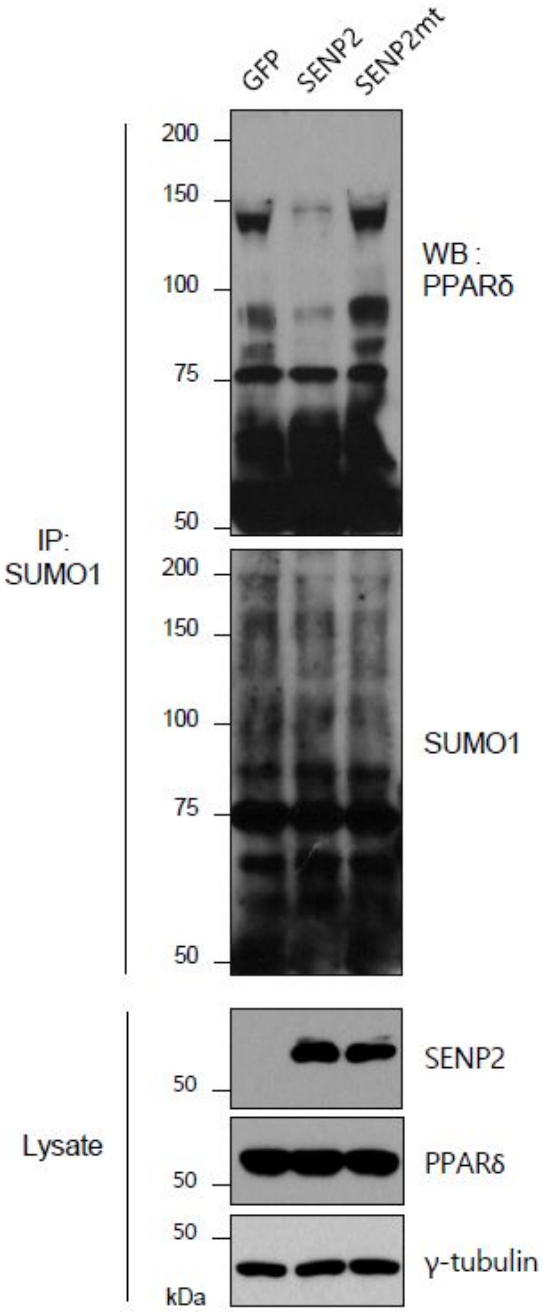
GFP
SENP2
SENP2mt
200
150
100
75
50
WB :
PPARδ
IP:
SUMO1
200
150
100
75
50
SUMO1
Lysate
50
SENP2
50
PPARδ
50
γ-tubulin
kDa

Figure 22. SENP2 stimulates deSUMOylation of endogenous PPARδ in C2C12 myotubes

C2C12 myotubes were infected with Ad-GFP, Ad-SENP2 and Ad-SENP2 mutant (50 moi). Cell lysates were subjected to immunoprecipitation with anti-SUMO1 antibody followed by immunoblot with anti-PPARδ and anti-SUMO1. The lysates were subjected to immunoblot with anti-SENP2, anti-PPARδ and anti-GAPDH.

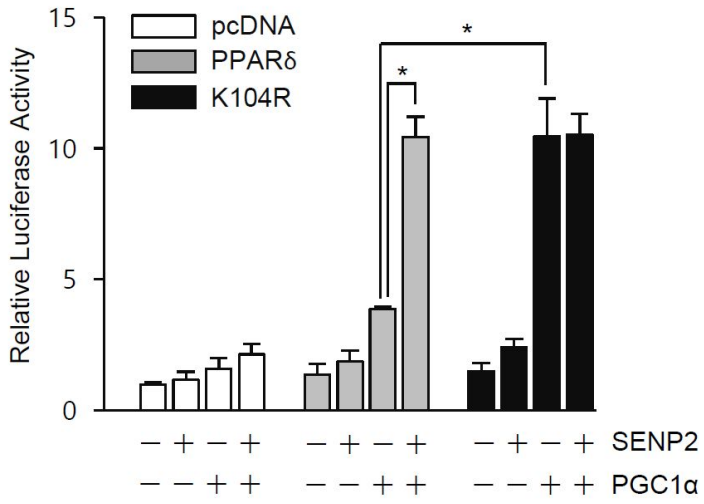

Figure 23. deSUMOylation of PPARδ by SENP2 increases transcriptional activity of PPARδ

COS7 cells were transfected with pTK-PPRE-luciferase (0.3 μg), pCMV-β-gal (0.1 μg), pcDNA-HA-PPARδ wild type or pcDNA-HA-PPARδ K104R mutant (0.1 μg), pFLAG-SUMO1 (0.1 μg), pHA-PGC1α and pFlag-SENP2 (0.1 μg). Luciferase activity was normalized by β–galactosidasse activity, and the value of the cells not transfected with PPARδ, SENP2 and PGC1α expression vectors was set to 1. n=5. (* = $p < 0.05$)

Generation of muscle specific SENP2 transgenic mice

Based on the microarray analysis, muscle specific SENP2 transgenic mice (referred to as mSENP2-TG mice) were generated. Muscle specific SENP2 transgenic mice by inserting the SENP2-FLAG construct to a β-globin gene cassette having the MCK promoter (Figure 24). Figure 24 is contributed by pf. YoungBum Kim in Harvard Medical School and pf. ByungChul Oh in Gachon University.

Generally, skeletal muscle is classified into five types of skeletal muscle, quadriceps muscle (QM), gastrocnemius muscle (GM), soleus muscle (SM), extensor digitorum longus muscle (EDL) and tibialis anterior muscle (TA). The SENP2-FLAG mRNA was expressed in all types of muscle tissues of mSENP2-TG mice but not in those of WT mice (Figure 25A). It was not expressed in the liver or epididymal fat tissues of both the mSENP2-TG and wild type mice (Figure 25B). Also, the SENP2 protein could be detected in the skeletal muscle of the mSENP2-TG mice but not in that of wild type mice (Figure 25C). In addition, the total protein level of SENP2 was about three fold higher in the muscle of mSENP2-TG mice than that of wild type mice under both chow- and high fat diet conditions (HFD). These results confirmed that SENP2 was overexpressed in the muscle of mSENP2-TG mice (Figure 25D).

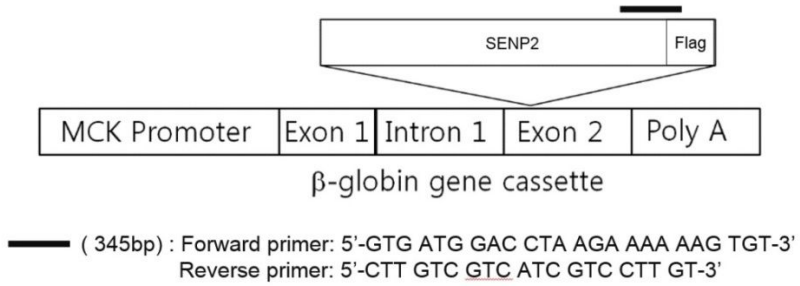

Figure 24. Plasmid construct for skeletal muscle SENP2 transgenic (mSENP2-TG) mice

The diagram shows the insertion of cDNA for SENP2-FLAG into the exon-2 of globin gene cassette for generation of mSENP2-TG mice. cDNAs encoding SENP2-FLAG were subcloned into a truncated β-globin expression vector. A 3.3 kb fragment of DNA isolated from the mouse muscle creatine kinase (MCK) promoter was subcloned into the upstream from exon 1 of the β-globin cassette. Microinjected mouse oocytes were introduced into pseudopregnant females. Transgenic offspring were identified originally by Southern analyses, and subsequent genotyping was by PCR. At least two independent lines were obtained, and each had the same phenotype.

(A)

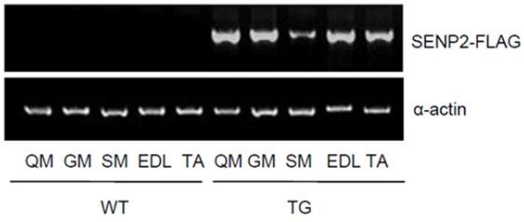
SENP2-FLAG
α-actin
QM GM SM EDL TA QM GM SM EDL TA
WT
TG

(B)

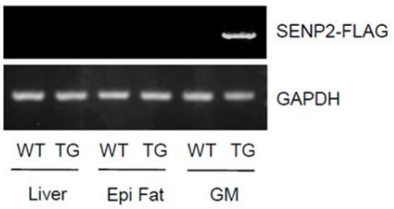
SENP2-FLAG
GAPDH
WT TG WT TG WT TG
Liver
Epi Fat
GM

(C)

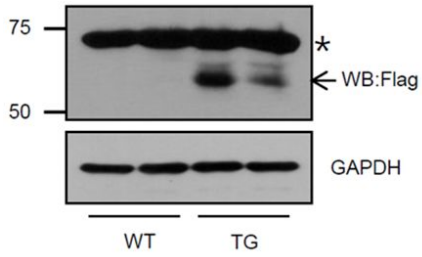
75
50
*
WB:Flag
GAPDH
WT
TG

(D)

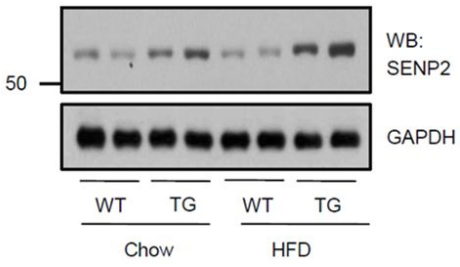
50
WB:
SENP2
GAPDH
WT TG WT TG
Chow
HFD

Figure 25. Comparison of SENP2 expression levels in both WT and mSENP2 TG mice

Total RNA was isolated from various types of muscle: (A) quadriceps (QM), gastrocnemius (GM), soleus (SM), extensor digitorum longus (EDL), and tibialis anterior (TA) of WT and mSENP2 TG mice. The RNA was subjected to RT-PCR using primers specific to SENP2-FLAG. (B) Experiments were performed as in Figure 3 A but using the liver, the epididymal fat (Epi Fat) and the GM. (C) Extracts were prepared from the GM of WT or mSENP2 TG mice and subjected to immunoblot with anti-FLAG antibody. (* : non-specific band) (D) Extracts were prepared from the gastrocnemius muscle of WT and mSENP2 TG mice that had been fed with chow or HFD. They were then subjected to immunoblot with anti-SENP2 antibody.

Metabolic phenotypes of muscle specific SENP2 transgenic mice

Body weight and fat mass of mSENP2-TG mice were significantly lower than those of WT mice under HFD conditions (Figure 26 A-C), whereas lean mass and bone mineral contents (BMC) of the mSENP2-TG mice were similar to those of WT mice (Figure 26D, 26E). Analysis of glucose tolerance tests (GTT) and insulin tolerance tests (ITT) showed improvement of glucose tolerance and insulin sensitivity in than mSENP2-TG mice under HFD condition (Figure 27A, 27B). Moreover, the basal levels of insulin and triglyceride in the serum of mSENP2-TG mice in HFD condition were much lower than those of WT mice (Figure 28A, 28B). On the other hand, little or no difference was detected in the total cholesterol , Low density lipoprotein (LDL), High density lipoprotein (HDL), aspartate aminotransferase (AST), alanine transferase (ALT) and muscle enzyme creatinine phosphokinase (CPK) under both chow and HFD conditions (Figure 28B). Figure 28 is contributed by pf. ByungChul Oh in Gachon University. Moreover, electron microscopic analysis revealed that the gastrocnemius muscle of the mSENP2-TG mice contained much lower fat than that of WT mice under HFD conditions (Figure 29). On the other hand, the fat level in the liver and

fat size of adipose tissues of the mSENP2-TG mice was similar to that of WT mice, respectively, under both chow and HFD conditions (Figure 30). Significantly, insulin-stimulated phosphorylation levels of inulin receptor substrate 1 (IRS1) and protein kinase B (PKB/Akt) in the gastrocnemius muscle of mSENP2-TG mice were much higher than those of WT mice under both chow and HFD conditions (Figure 31), suggesting that SENP2 overexpression improves insulin signaling pathway. These results indicate that SENP2 overexpression in skeletal muscle alleviates HFD-induced obesity and insulin resistance.

Next, I determined the levels of ATP in the gastrocnemius muscle. The ATP levels of mSENP2-TG mice were about 1.5 folds higher than that of WT mice under HFD condition (Figure 32). Also I checked the levels of free fatty acid and triglyceride in the gastrocnemius muscle. While the level of free fatty acids in the muscle tissue of the mSENP2-TG mice was similar to that of WT mice, the triglyceride level in the mSENP2-TG mice was significantly lower than that of WT mice under both chow and HFD conditions (Figure 33). In addition, FAO was markedly increased in the muscle of the mSENP2-TG mice under both chow and HFD conditions as compared to that of WT mice (Figure 34). These results indicate that the muscle tissues of the mSENP2-TG mice show higher FAO, which would

reduce fat accumulation. So, I examined the changes of fatty acid oxidation-related genes [(Acyl-CoA Synthetase Long-Chain Family Member 1(ACSL1), Carnitine palmitoyltransferase I (CPT1b), Mitochondrial uncoupling protein 3 (UCP3), cluster of differentiation 36 (CD36), fatty acid binding protein3 (FABP3), Medium-chain acyl-CoA dehydrogenase (MCAD) and acetyl-Coenzyme A acyltransferase 2 (Acaa2)], transcription factors (PPARα, PPARδ, PPARγ, PGC1α and KLF5) and mitochondrial biogenesis related genes (mtTFA and NRF1). mRNA levels of FAO-associated enzyme genes such as ACSL1, CPT1b and UCP3 were higher in the gastrocnemius muscle of HFD fed TG mice than that of WT mice (Figure 35). However, no apparent difference between mSENP2-TG and WT mice muscles was observed in the mRNA levels of transcriptional factors, including PPARα, PPARδ, PPARγ, PGC1α and KLF5 in both chow and HFD conditions (Figure 35). Also, mRNA levels of mitochondrial biogenesis-related genes including mtTFA and NRF1 were not significantly changed in TG mice in both chow and HFD conditions (Figure 35). Collectively, these results suggest that SENP2 plays a critical role in the increase of FAO by inducing the expression of FAO-related enzymes and SENP2 overexpression in muscle alleviates HFD-induced obesity and insulin resistance.

(A)

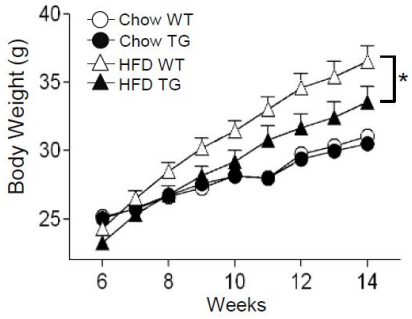
Chow WT
Chow TG
HFD WT
HFD TG
Body Weight (g)
40
35
30
25
6
8
10
12
14
Weeks
*

(B)

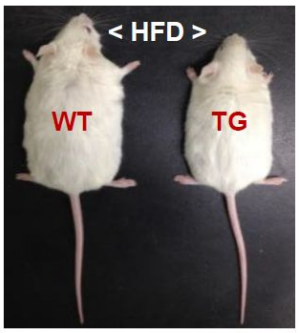
< HFD >
WT
TG

(C)

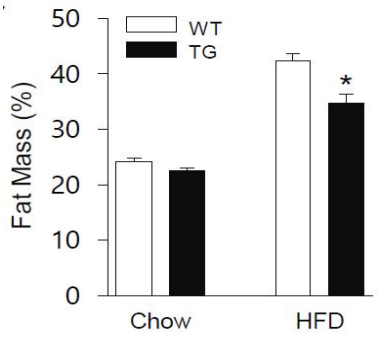
WT
TG
Fat Mass (%)
50
40
30
20
10
0
*
Chow
HFD

(D)

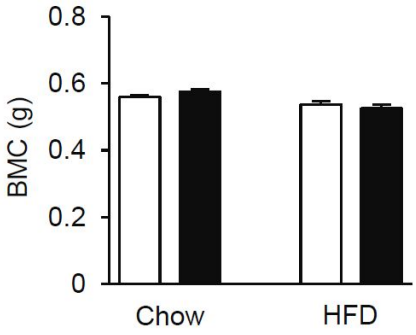
BMC (g)
0.8
0.6
0.4
0.2
0
Chow
HFD

(E)

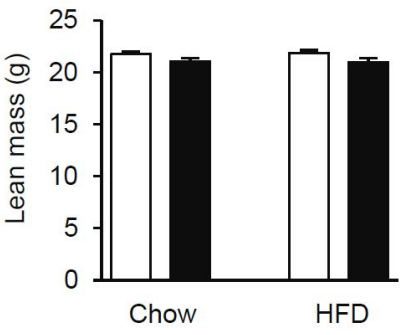
Lean mass (g)
25
20
15
10
5
0
Chow
HFD

Figure 26. SENP2 overexpression decreases fat mass and body weight, but does not have an effect on lean mass and bone mineral content

WT and mSENP2-TG mice were fed with chow or HFD. The composition of HFD is high sucrose 60% HFD. (A) Their body weights were measured every day for 14 weeks (n = 15-20/group). (B) An example of the size difference between WT and mSENP2-TG mice after HFD feeding was shown. (C) Body fat mass was measured after feeding the mice with chow or HFD for 8 weeks. (D, E) Also, BMC (bone mineral content) and lean mass were measured after feeding the mice with chow or HFD for 8 weeks.

(* = $p < 0.05$ *vs* HFD WT)

(A) (B)

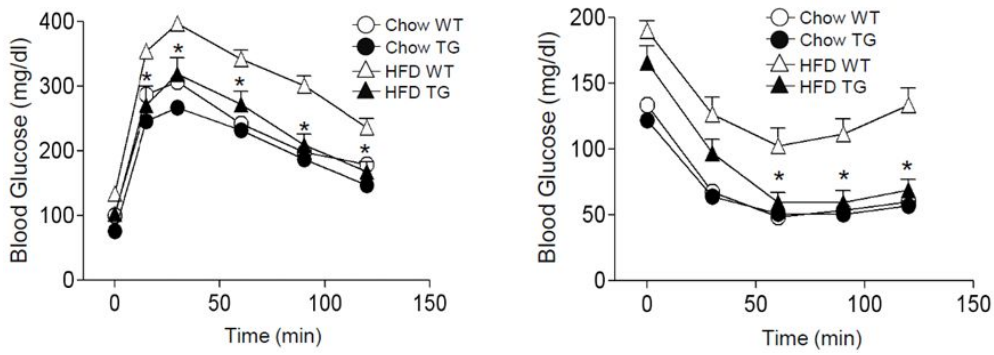

Figure 27. Glucose tolerance and insulin resistance are improved by SENP2

(A) Glucose tolerance test and (B) insulin tolerance test were performed in chow and HFD conditions. (n = 24/group). (A) For glucose tolerance test, mice were fasted for 16 h and injected 1 g/kg of glucose. (B) In insulin tolerance test, the mice were fasted 6 h and injected 1 unit/kg of insulin. (* = $p < 0.05$ *vs* HFD WT)

(A)

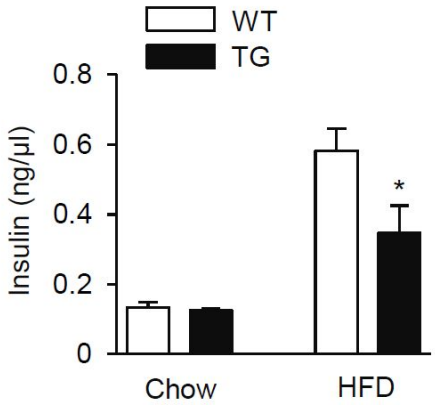
WT
TG
Insulin (ng/μl)
0.8
0.6
0.4
0.2
0
*
Chow
HFD

(B)

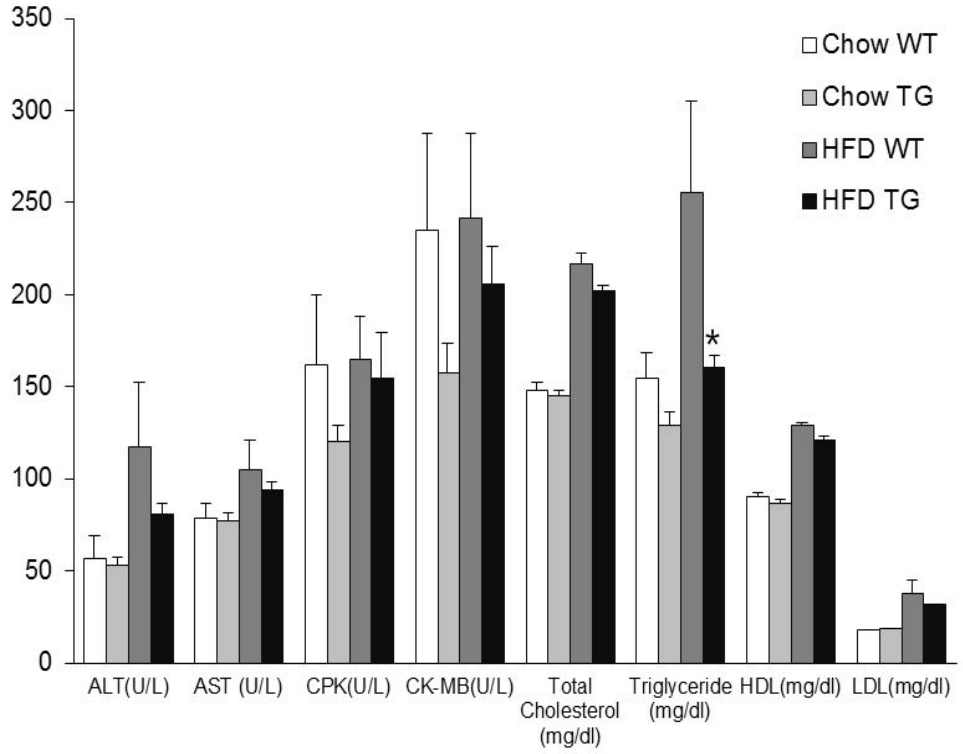
350
300
250
200
150
100
50
0
Chow WT
Chow TG
HFD WT
HFD TG
*
ALT(U/L)
AST (U/L)
CPK(U/L)
CK-MB(U/L)
Total Cholesterol (mg/dl)
Triglyceride (mg/dl)
HDL(mg/dl)
LDL(mg/dl)

Figure 28. Serum analysis of WT and mSENP2-TG mice in chow and high fat diet (HFD) conditions

Insulin, total Cholesterol, Low density lipoprotein (LDL), High density lipoprotein (HDL), Triglycerides, aspartate aminotransferase (AST), alanine transferase (ALT), muscle enzyme creatinine phosphokinase (CPK) levels were measured in the serum of WT and mSENP2-TG mice in chow and HFD conditions (A, B). Chow WT (n=15), Chow TG (n=12), HFD WT (n=13), HFD TG (n=11). (* = $p < 0.05$ *vs* HFD WT)

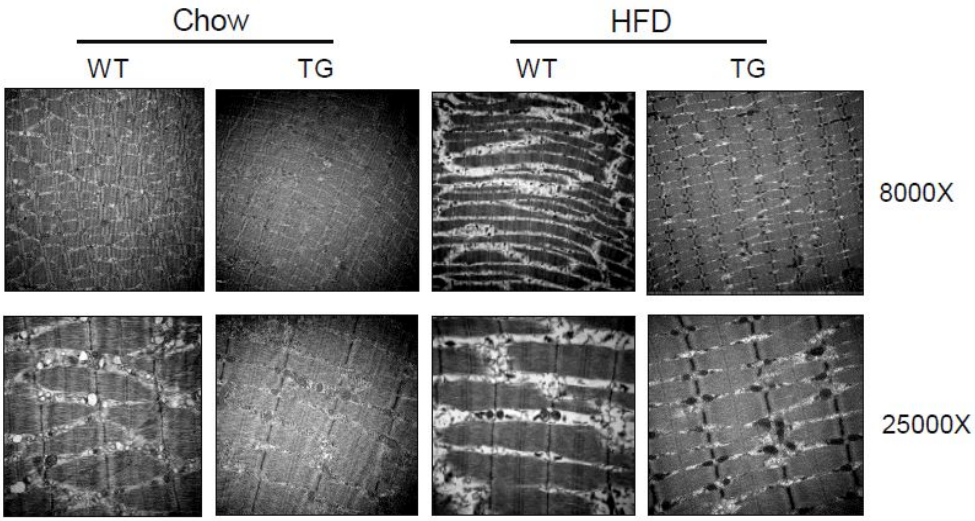

Figure 29. SENP2 overexpression decreases lipid accumulation and increases mitochondria biogenesis

Sections of gastrocnemius muscle tissues were obtained, and then subjected to electron microscopy. Lipid droplets (white) and mitochondria (black) were shown.

(A)

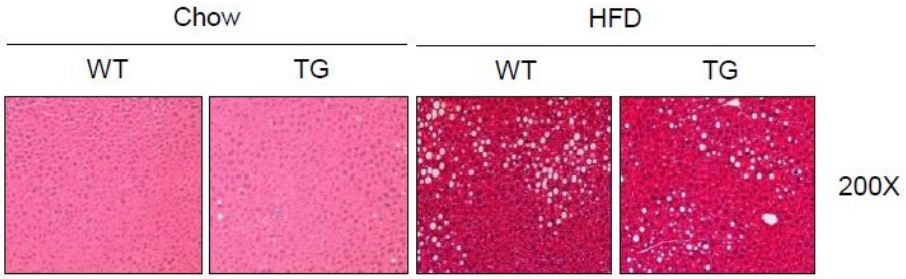

(B)

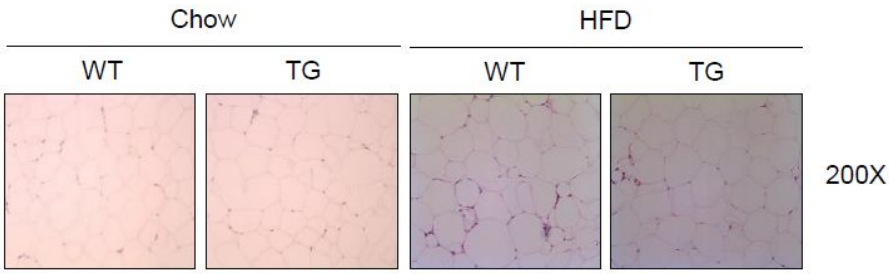

Figure 30. H&E staining analysis of liver and white adipose tissue of WT and mSENP2-TG mice

Sections of (A) liver and (B) WAT were obtained, and then subjected to H&E staining. After stain, the slide samples were observed with 200 magnification using microscope.

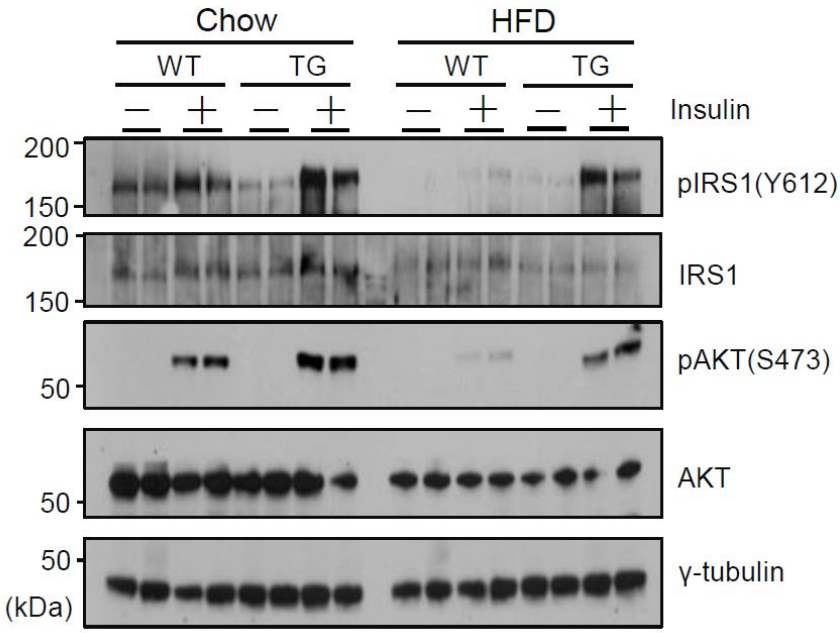

Figure 31. SENP2 improves insulin signaling pathway

For activation of insulin signaling pathway in WT and mSENP2-TG mice, the mice were injected with insulin (1 unit/kg) 15 min before sacrifice. Lysates (15 μg) of gastrocnemius muscle of WT and mSENP2-TG mice in chow and HFD conditions were subjected to immunoblot analysis using an anti-pIRS1, anti-IRS1, anti-pAKT and anti-AKT.

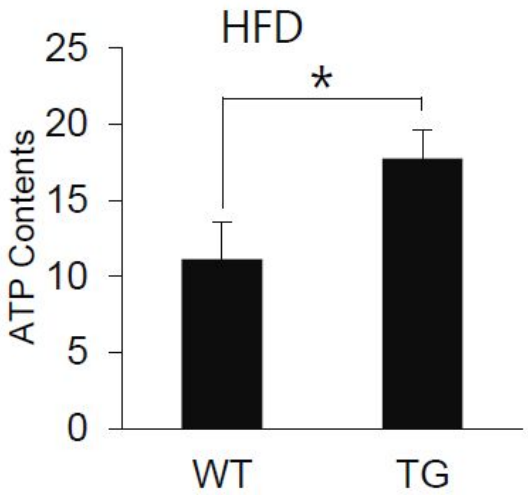

Figure 32. SENP2 increases ATP contents in HFD conditions

ATP contents were measured from gastrocnemius muscle of WT and mSENP2-TG mice in HFD condition. Gastrocnemius muscle was lysed in a commercial lysis buffer, and then the lysate (150 μl) was subjected to VICTOR3 with the substrate (50 μl). Absolute values of ATP were normalized by protein concentration. Chow WT (n=9), Chow TG (n=7), HFD WT (n=10), HFD TG (n=8). (* = $p < 0.05$ *vs* WT)

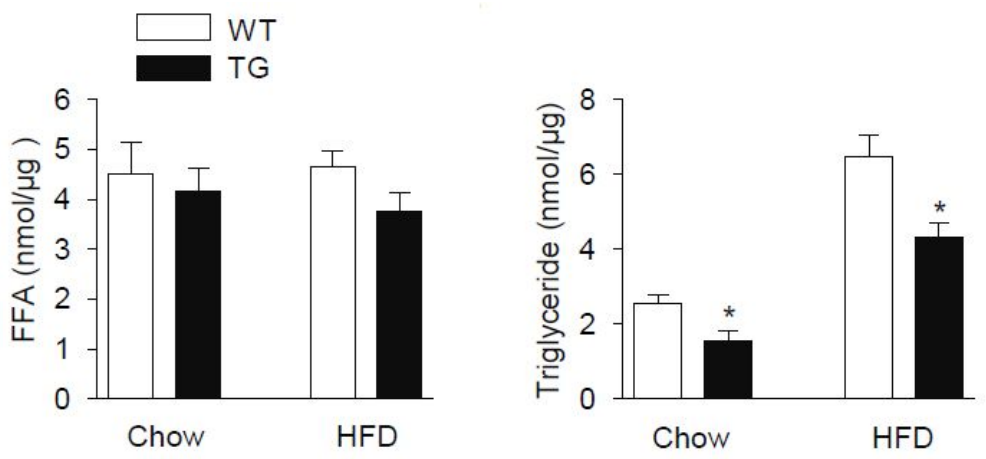

Figure 33. The levels of FFA and triglyceride in gastrocnemius muscle.

Total lipid was extracted from gastrocnemius muscle of WT and mSENP2-TG mice in chow and HFD conditions. Free fatty acid and triglyceride in the total lipid were measured using NEFA kit and WACO kit, respectively. Absolute values of FFA and triglyceride were normalized weight of gastrocnemius muscle. Chow WT (n=8), Chow TG (n=8), HFD WT (n=8), HFD TG (n=8). (* = $p < 0.05$ *vs* Chow and HFD WT)

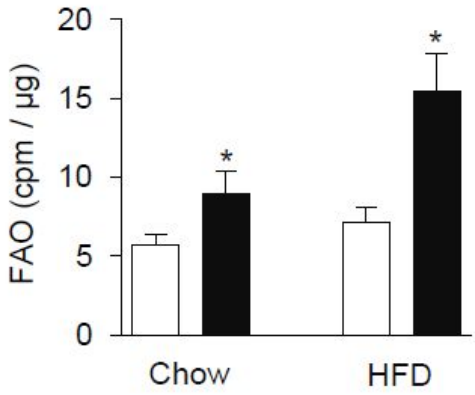

Figure 34. SENP2 increases fatty acid oxidation (FAO) in skeletal muscle tissue.

WT and mSENP2-TG mice were fed with chow or HFD for 12 weeks. Lysate of gastrocnemius muscle of WT and mSENP2-TG was measured fatty acid oxidation. Fatty acid oxidation was used to measure by incubation with C^{14}-palmitate in the reaction buffer for 2h. CPM values were normalized by protein contents. Chow WT (n=8), Chow TG (n=8), HFD WT (n=8), HFD TG (n=8). (* = $p < 0.05$ *vs* Chow and HFD WT)

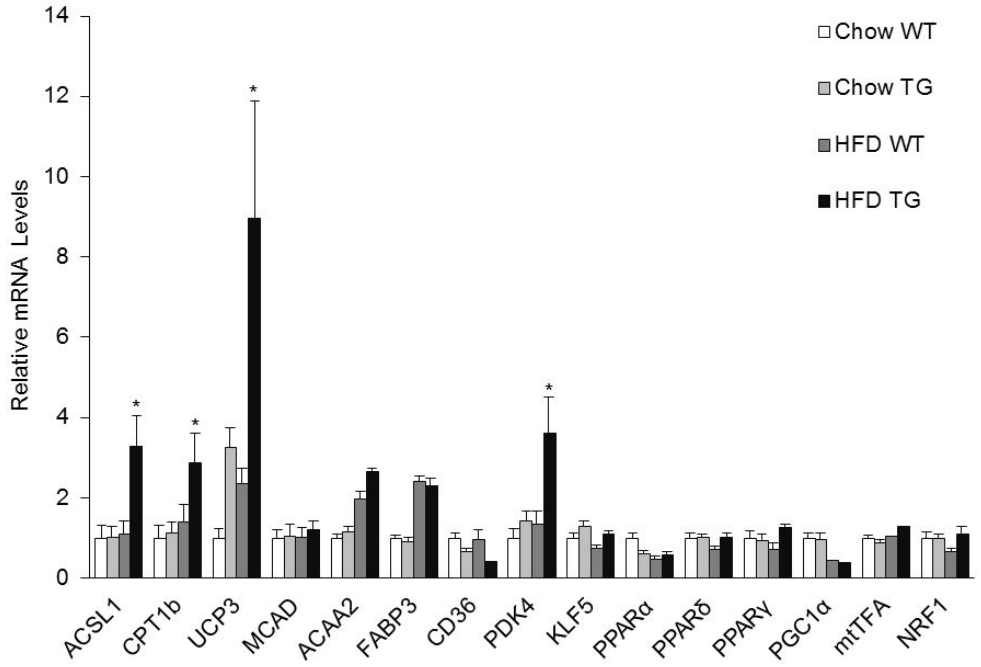

Figure 35. Effects of SENP2 overexpression on RNA levels of various genes in skeletal muscle

Total RNA was extracted from gastrocnemius muscle of WT and mSENP2-TG mice in chow and HFD conditions. The RNA (1 ug) subjected to real-time PCR using primers for fatty acid oxidation-related genes, transcription factors and mitochondrial biogenesis-related genes. Chow WT (n=14), Chow TG (n=14), HFD WT (n=12), HFD TG (n=12). (* = $p < 0.05$ *vs* HFD WT)

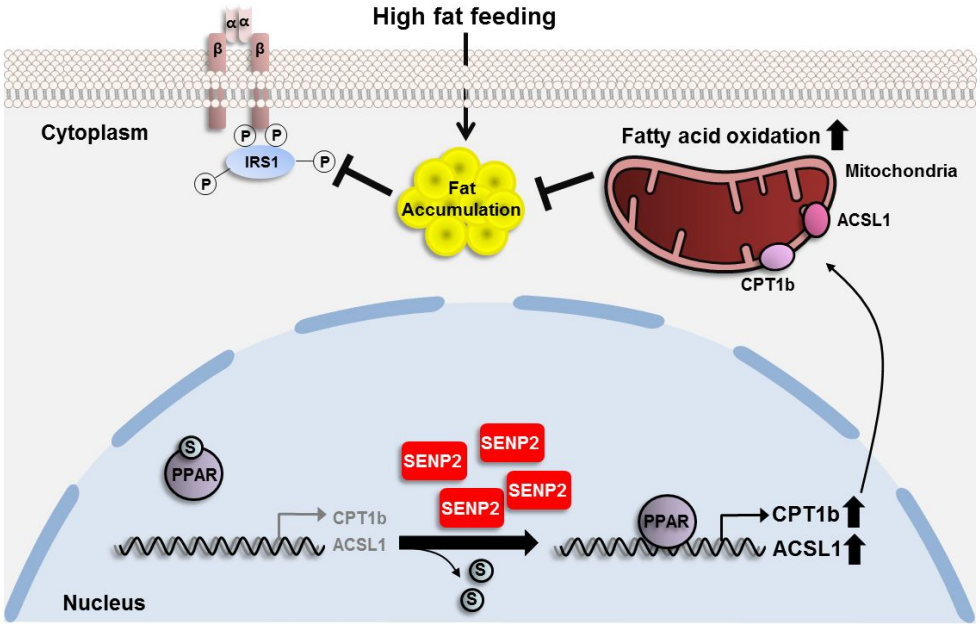

Figure 36. Control of fatty acid metabolism by SENP2 overexpression

DISCUSSION

There are some reports to show the roles of SENP2 in the adipocyte and some cancer cell line. However, any role of SENP2 in the skeletal muscle metabolism has not been revealed. To figure out the metabolic role of SENP2 overexpression in skeletal muscle, I started this study from the microarray analysis with RNA samples in which SENP2 overexpressed in C2C12 myotubes. When SENP2 overexpressed in C2C12 myotubes, mRNA levels of the genes related to glucose metabolic process, fatty acid metabolism, muscle cell differentiation, calcium ion transport and glucose transport were up-regulated versus control (Figure 13A). On the other hand, mRNA levels of the genes related to cell cycle, DNA replication, chromosome organization, cytoskeleton organization, RNA processing and ribosome biogenesis were down-regulated versus control (Figure 13A). These results could be an important clues on lipid metabolism effects by SENP2 overexpression in C2C12 myotubes. However, further study on the role of the other up-regulated pathways, which are glucose metabolic process and glucose transport, by SENP2 overexpression is required.

SENP2 overexpression by adeno-virus is increase fatty acid oxidation and

expression levels of fatty acid oxidation associated genes in C2C12 myotubes (Figure 14). SENP2 overexpression leads to deSUMOylation of PPARδ and PPARγ and deSUMOylated PPARδ and PPARγ bind to on the promoter regions of fatty acid oxidation associated genes (Figure 15-20). At this point, SUMOylation of PPARδ is very interesting data (Figure 19, 20). There was no report about SUMOylation of PPARδ until this study. These results indicated that SENP2 overexpression increase fatty acid oxidation and expression levels of fatty acid oxidation associated genes via PPARδ and PPARγ in C2C12 myotubes. In the muscle of mSENP2 TG mice, SENP2 overexpression decreased body weight, fat mass and increased FAO levels and expression of FAO-associated genes (Figure 26, 34, 35). Also, SENP2 overexpression improved glucose tolerance, insulin resistance and insulin signaling pathway under HFD condition (Figure 27, 31). These findings demonstrate that SENP2 is a crucial factor on lipid metabolism in skeletal muscle.

However, some questions were raised from the results of this study. First question is from electron microscope data and mRNA level data of mitochondria biogenesis associated genes. Mitochondrial mass were increased by SENP2 in electron microscope data, but there is no big difference in the expression levels of mitochondrial biogenesis-associated

genes such as mtTFA and NRF1. The question is how mitochondria mass were increased in mSENP2 TG mice. Recently, it was reported that mitochondrial biogenesis is regulated through deSUMOylation of PGC-1α by SENP1 [73]. To solve this question, further study on the mitochondrial biogenesis by SENP2 is required.

Second question is why SENP2-induced FAO is not observed in HFD-fed wild type mice. In chapter I, in vitro C2C12 myotubes culture system, palmitate efficiently induces SENP2 expression, which increases FAO (Figure 1, 2, 9). Either FAO or the mRNA levels of ACSL1 and CPT1b are not significantly changed by HFD (Figure 34, 35). The reasons or the different results in these models could derive from other metabolic disturbances associated with chronic high-fat feeding or from different experimental systems (in vitro vs, in vivo). Future studies will need to clarify these important issues.

Third question is whether PPARδ and PPARγ are only direct targets of SENP2 to promote FAO in muscle. Knockdown of PPARδ or PPARγ efficiently, but not completely, suppresses SENP2-mediated FAO (Figure 16B). These observations could explain the possibility that SENP2 regulates the function FAO-associated enzymes through direct modification. It is also possible that SENP2 controls the expression or function of another protein(s)

that is important for FAO but not tested in this study. Nevertheless, this study clearly show that SENP2 increases FAO mainly by promoting PPARδ- and PPARγ- mediated expression of FAO-associated enzymes.

While SUMOylation of PPARγ was previously reported, we show for the first time that PPARδ is SUMOylated in this study. Final question is existence of high-molecular weight SUMOylated bands of PPARδ (Figure 19, 20). However, it is unlikely that PPARδ is SUMOylated at multiple sites because its K104R mutation completely abrogated PPARδ SUMOylation. The facts that SUMO1 is known to be incapable of forming a polymeric chain and our result showing that ubiquitination of PPARδ is increased by SUMOylation suggest that the high-molecular weight bands consist of PPARδ modified by both SUMO1 and ubiquitin. In fact, there are several reports that SUMOylation of proteins promotes their ubiquitination [106-108]. Further study will determine whether the ubiquitination is linked to proteasome-mediated degradation of PPARδ.

PPARδ is more abundant than PPARγ in muscle, suggesting that the contribution of PPARδ in lipid metabolism in muscle could be greater than that of PPARγ. Interestingly, however, the effect of PPARγ on gene expression of FAO-associated enzymes and in turn on FAO in C2C12 myotubes was nearly similar to that of PPARδ (Figure 16B, 16C). Thus, it

appears that PPARγ, in addition to PPARδ, plays an important role in lipid metabolism in skeletal muscle. This is further supported by experimental evidences showing that muscle-specific deletion of PPARγ results in insulin resistance and promotes adiposity [109, 110].

Important finding of this study is to figure out lipid metabolism regulation by SENP2 in skeletal muscle. SENP2 overexpression in the skeletal muscle increases fat burning by increase of fatty acid oxidation-associated gene-expression by deSUMOylation of transcription factors. These results clearly showed that SENP2 plays an important role on lipid metabolism in the skeletal muscle. Furthermore, SENP2 could be a novel therapeutic target, such as SENP2 agonist or SUMO1 inhibitor, for the treatment of obesity-linked metabolic disorders.

Reference

1. McKinlay, J. and L. Marceau, *US public health and the 21st century: diabetes mellitus.* Lancet, 2000. **356**(9231): p. 757-61.
2. Ritz, P. and G. Berrut, *Mitochondrial function, energy expenditure, aging and insulin resistance.* Diabetes Metab, 2005. **31 Spec No 2**: p. 5s67-5s73.
3. Choi, C.S., et al., *Paradoxical effects of increased expression of PGC-1alpha on muscle mitochondrial function and insulin-stimulated muscle glucose metabolism.* Proc Natl Acad Sci U S A, 2008. **105**(50): p. 19926-31.
4. Koves, T.R., et al., *Mitochondrial overload and incomplete fatty acid oxidation contribute to skeletal muscle insulin resistance.* Cell Metab, 2008. **7**(1): p. 45-56.
5. Wang, S., et al., *Increased fatty acid oxidation in transgenic mice overexpressing UCP3 in skeletal muscle.* Diabetes Obes Metab, 2003. **5**(5): p. 295-301.
6. Barja, G., *Mitochondrial oxygen radical generation and leak: sites of production in states 4 and 3, organ specificity, and relation to aging and longevity.* J Bioenerg Biomembr, 1999. **31**(4): p. 347-66.
7. Turrens, J.F., *Mitochondrial formation of reactive oxygen species.* J Physiol,

2003. **552**(Pt 2): p. 335-44.

8. Turrens, J.F. and A. Boveris, *Generation of superoxide anion by the NADH dehydrogenase of bovine heart mitochondria.* Biochem J, 1980. **191**(2): p. 421-7.

9. Turrens, J.F., A. Alexandre, and A.L. Lehninger, *Ubisemiquinone is the electron donor for superoxide formation by complex Ⅲ of heart mitochondria.* Arch Biochem Biophys, 1985. **237**(2): p. 408-14.

10. Cadenas, E., et al., *Production of superoxide radicals and hydrogen peroxide by NADH-ubiquinone reductase and ubiquinol-cytochrome c reductase from beef-heart mitochondria.* Arch Biochem Biophys, 1977. **180**(2): p. 248-57.

11. Powers, S.K. and M.J. Jackson, *Exercise-induced oxidative stress: cellular mechanisms and impact on muscle force production.* Physiol Rev, 2008. **88**(4): p. 1243-76.

12. Kliewer, S.A., et al., *Retinoid X receptor interacts with nuclear receptors in retinoic acid, thyroid hormone and vitamin D3 signalling.* Nature, 1992. **355**(6359): p. 446-9.

13. Olefsky, J.M. and A.R. Saltiel, *PPAR gamma and the treatment of insulin resistance.* Trends Endocrinol Metab, 2000. **11**(9): p. 362-8.

14. Ho, J.N., et al., *Anti-obesity effects of germinated brown rice extract through down-regulation of lipogenic genes in high fat diet-induced*

obese mice. Biosci Biotechnol Biochem, 2012. **76**(6): p. 1068-74.

15. Zandbergen, F., et al., *The G0/G1 switch gene 2 is a novel PPAR target gene.* Biochem J, 2005. **392**(Pt 2): p. 313-24.

16. Wang, Y.X., et al., *Peroxisome-proliferator-activated receptor delta activates fat metabolism to prevent obesity.* Cell, 2003. **113**(2): p. 159-70.

17. Rosen, E.D., et al., *PPAR gamma is required for the differentiation of adipose tissue in vivo and in vitro.* Mol Cell, 1999. **4**(4): p. 611-7.

18. Wang, F., et al., *Lipoatrophy and severe metabolic disturbance in mice with fat-specific deletion of PPARgamma.* Proc Natl Acad Sci U S A, 2013. **110**(46): p. 18656-61.

19. Poulsen, L., M. Siersbaek, and S. Mandrup, *PPARs: fatty acid sensors controlling metabolism.* Semin Cell Dev Biol, 2012. **23**(6): p. 631-9.

20. Barbera, M.J., et al., *Peroxisome proliferator-activated receptor alpha activates transcription of the brown fat uncoupling protein-1 gene. A link between regulation of the thermogenic and lipid oxidation pathways in the brown fat cell.* J Biol Chem, 2001. **276**(2): p. 1486-93.

21. Braissant, O., et al., *Differential expression of peroxisome proliferator-activated receptors (PPARs): tissue distribution of PPAR-alpha, -beta, and -gamma in the adult rat.* Endocrinology, 1996. **137**(1): p. 354-66.

22. Escher, P., et al., *Rat PPARs: quantitative analysis in adult rat tissues and regulation in fasting and refeeding.* Endocrinology, 2001. **142**(10): p.

4195-202.

23. Johnson, E.S., *Protein modification by SUMO.* Annu Rev Biochem, 2004. **73**: p. 355-82.

24. Seeler, J.S. and A. Dejean, *Nuclear and unclear functions of SUMO.* Nat Rev Mol Cell Biol, 2003. **4**(9): p. 690-9.

25. Li, S.J. and M. Hochstrasser, *A new protease required for cell-cycle progression in yeast.* Nature, 1999. **398**(6724): p. 246-51.

26. Colby, T., et al., *SUMO-conjugating and SUMO-deconjugating enzymes from Arabidopsis.* Plant Physiol, 2006. **142**(1): p. 318-32.

27. Gill, G., *SUMO and ubiquitin in the nucleus: different functions, similar mechanisms?* Genes Dev, 2004. **18**(17): p. 2046-59.

28. Bailey, D. and P. O'Hare, *Characterization of the localization and proteolytic activity of the SUMO-specific protease, SENP1.* J Biol Chem, 2004. **279**(1): p. 692-703.

29. Hang, J. and M. Dasso, *Association of the human SUMO-1 protease SENP2 with the nuclear pore.* J Biol Chem, 2002. **277**(22): p. 19961-6.

30. Zhang, H., H. Saitoh, and M.J. Matunis, *Enzymes of the SUMO modification pathway localize to filaments of the nuclear pore complex.* Mol Cell Biol, 2002. **22**(18): p. 6498-508.

31. Di Bacco, A., et al., *The SUMO-specific protease SENP5 is required for cell division.* Mol Cell Biol, 2006. **26**(12): p. 4489-98.

32. Gong, L. and E.T. Yeh, *Characterization of a family of nucleolar SUMO-specific proteases with preference for SUMO-2 or SUMO-3.* J Biol Chem, 2006. **281**(23): p. 15869-77.

33. Nishida, T., H. Tanaka, and H. Yasuda, *A novel mammalian Smt3-specific isopeptidase 1 (SMT3IP1) localized in the nucleolus at interphase.* Eur J Biochem, 2000. **267**(21): p. 6423-7.

34. Mukhopadhyay, D., et al., *SUSP1 antagonizes formation of highly SUMO2/3-conjugated species.* J Cell Biol, 2006. **174**(7): p. 939-49.

35. Ohshima, T., H. Koga, and K. Shimotohno, *Transcriptional activity of peroxisome proliferator-activated receptor gamma is modulated by SUMO-1 modification.* J Biol Chem, 2004. **279**(28): p. 29551-7.

36. Floyd, Z.E. and J.M. Stephens, *Control of peroxisome proliferator-activated receptor gamma2 stability and activity by SUMOylation.* Obes Res, 2004. **12**(6): p. 921-8.

37. Yamashita, D., et al., *The transactivating function of peroxisome proliferator-activated receptor gamma is negatively regulated by SUMO conjugation in the amino-terminal domain.* Genes Cells, 2004. **9**(11): p. 1017-29.

38. Haffner, S.M., et al., *Effect of rosiglitazone treatment on nontraditional markers of cardiovascular disease in patients with type 2 diabetes mellitus.* Circulation, 2002. **106**(6): p. 679-84.

39. Li, A.C., et al., *Peroxisome proliferator-activated receptor gamma ligands inhibit development of atherosclerosis in LDL receptor-deficient mice.* J Clin Invest, 2000. **106**(4): p. 523-31.

40. Perissi, V., et al., *A corepressor/coactivator exchange complex required for transcriptional activation by nuclear receptors and other regulated transcription factors.* Cell, 2004. **116**(4): p. 511-26.

41. Ogawa, S., et al., *A nuclear receptor corepressor transcriptional checkpoint controlling activator protein 1-dependent gene networks required for macrophage activation.* Proc Natl Acad Sci U S A, 2004. **101**(40): p. 14461-6.

42. Hoberg, J.E., F. Yeung, and M.W. Mayo, *SMRT derepression by the IkappaB kinase alpha: a prerequisite to NF-kappaB transcription and survival.* Mol Cell, 2004. **16**(2): p. 245-55.

43. Zelcer, N. and P. Tontonoz, *SUMOylation and PPARgamma: wrestling with inflammatory signaling.* Cell Metab, 2005. **2**(5): p. 273-5.

44. Oishi, Y., et al., *SUMOylation of Kruppel-like transcription factor 5 acts as a molecular switch in transcriptional programs of lipid metabolism involving PPAR-delta.* Nat Med, 2008. **14**(6): p. 656-66.

45. Jennewein, C., et al., *Sumoylation of peroxisome proliferator-activated receptor gamma by apoptotic cells prevents lipopolysaccharide-induced NCoR removal from kappaB binding sites mediating transrepression of*

proinflammatory cytokines. J Immunol, 2008. **181**(8): p. 5646-52.

46. Jiang, M., S.Y. Chiu, and W. Hsu, *SUMO-specific protease 2 in Mdm2-mediated regulation of p53.* Cell Death Differ, 2011. **18**(6): p. 1005-15.

47. Chen, C.H., et al., *SENP1 deSUMOylates and regulates Pin1 protein activity and cellular function.* Cancer Res, 2013. **73**(13): p. 3951-62.

48. McMillan, L.E., et al., *Profiles of SUMO and ubiquitin conjugation in an Alzheimer's disease model.* Neurosci Lett, 2011. **502**(3): p. 201-8.

49. Qi, J., et al., *Differential expression and cellular localization of novel isoforms of the tendon biomarker tenomodulin.* J Appl Physiol (1985), 2012. **113**(6): p. 861-71.

50. Choi, H.K., et al., *Reversible SUMOylation of TBL1-TBLR1 regulates beta-catenin-mediated Wnt signaling.* Mol Cell, 2011. **43**(2): p. 203-16.

51. Ferdaoussi, M., et al., *Isocitrate-to-SENP1 signaling amplifies insulin secretion and rescues dysfunctional beta cells.* J Clin Invest, 2015. **125**(10): p. 3847-60.

52. Shao, L., et al., *SENP1-mediated NEMO deSUMOylation in adipocytes limits inflammatory responses and type-1 diabetes progression.* Nat Commun, 2015. **6**: p. 8917.

53. Chung, S.S., et al., *Control of adipogenesis by the SUMO-specific protease SENP2.* Mol Cell Biol, 2010. **30**(9): p. 2135-46.

54. Chung, S.S., et al., *SUMO modification selectively regulates transcriptional*

activity of peroxisome-proliferator-activated receptor gamma in C2C12 myotubes. Biochem J, 2011. **433**(1): p. 155-61.

55. Cheng, A.M., et al., *Apolipoprotein A-I attenuates palmitate-mediated NF-kappaB activation by reducing Toll-like receptor-4 recruitment into lipid rafts.* PLoS One, 2012. **7**(3): p. e33917.

56. Maloney, E., et al., *Activation of NF-kappaB by palmitate in endothelial cells: a key role for NADPH oxidase-derived superoxide in response to TLR4 activation.* Arterioscler Thromb Vasc Biol, 2009. **29**(9): p. 1370-5.

57. Kleinridders, A., et al., *MyD88 signaling in the CNS is required for development of fatty acid-induced leptin resistance and diet-induced obesity.* Cell Metab, 2009. **10**(4): p. 249-59.

58. Tsukumo, D.M., et al., *Loss-of-function mutation in Toll-like receptor 4 prevents diet-induced obesity and insulin resistance.* Diabetes, 2007. **56**(8): p. 1986-98.

59. Arancibia, S.A., et al., *Toll-like receptors are key participants in innate immune responses.* Biol Res, 2007. **40**(2): p. 97-112.

60. Lee, S.M., et al., *Involvement of the TLR4 (Toll-like receptor4) signaling pathway in palmitate-induced INS-1 beta cell death.* Mol Cell Biochem, 2011. **354**(1-2): p. 207-17.

61. Senn, J.J., *Toll-like receptor-2 is essential for the development of palmitate-induced insulin resistance in myotubes.* J Biol Chem, 2006.

281(37): p. 26865-75.

62. Davis, J.E., et al., *Absence of Tlr2 protects against high-fat diet-induced inflammation and results in greater insulin-stimulated glucose transport in cultured adipocytes.* J Nutr Biochem, 2011. **22**(2): p. 136-41.

63. Huang, S., et al., *Saturated fatty acids activate TLR-mediated proinflammatory signaling pathways.* J Lipid Res, 2012. **53**(9): p. 2002-13.

64. Jang, H.J., et al., *Toll-like receptor 2 mediates high-fat diet-induced impairment of vasodilator actions of insulin.* Am J Physiol Endocrinol Metab, 2013. **304**(10): p. E1077-88.

65. Cao, A., et al., *Long chain acyl-CoA synthetase-3 is a molecular target for peroxisome proliferator-activated receptor delta in HepG2 hepatoma cells.* J Biol Chem, 2010. **285**(22): p. 16664-74.

66. Song, S., et al., *Peroxisome proliferator activated receptor alpha (PPARalpha) and PPAR gamma coactivator (PGC-1alpha) induce carnitine palmitoyltransferase IA (CPT-1A) via independent gene elements.* Mol Cell Endocrinol, 2010. **325**(1-2): p. 54-63.

67. Nolan, C.J., et al., *Beta cell compensation for insulin resistance in Zucker fatty rats: increased lipolysis and fatty acid signalling.* Diabetologia, 2006. **49**(9): p. 2120-30.

68. Gao, X., et al., *Tetramethylpyrazine protects palmitate-induced oxidative damage and mitochondrial dysfunction in C2C12 myotubes.* Life Sci,

2011. **88**(17-18): p. 803-9.

69. Jheng, H.F., et al., *Mitochondrial fission contributes to mitochondrial dysfunction and insulin resistance in skeletal muscle.* Mol Cell Biol, 2012. **32**(2): p. 309-19.

70. Taheripak, G., et al., *Protein tyrosine phosphatase 1B inhibition ameliorates palmitate-induced mitochondrial dysfunction and apoptosis in skeletal muscle cells.* Free Radic Biol Med, 2013. **65**: p. 1435-46.

71. Fu, J., et al., *Disruption of SUMO-specific protease 2 induces mitochondria mediated neurodegeneration.* PLoS Genet, 2014. **10**(10): p. e1004579.

72. Heo, K.S., et al., *Disturbed flow-activated p90RSK kinase accelerates atherosclerosis by inhibiting SENP2 function.* J Clin Invest, 2015. **125**(3): p. 1299-310.

73. Cai, R., et al., *SUMO-specific protease 1 regulates mitochondrial biogenesis through PGC-1alpha.* J Biol Chem, 2012. **287**(53): p. 44464-70.

74. Yang, X., et al., *Saturated fatty acids enhance TLR4 immune pathways in human trophoblasts.* Hum Reprod, 2015. **30**(9): p. 2152-9.

75. Yuzefovych, L., G. Wilson, and L. Rachek, *Different effects of oleate vs. palmitate on mitochondrial function, apoptosis, and insulin signaling in L6 skeletal muscle cells: role of oxidative stress.* Am J Physiol Endocrinol Metab, 2010. **299**(6): p. E1096-105.

76. Heo, K.S., et al., *De-SUMOylation enzyme of sentrin/SUMO-specific protease 2 regulates disturbed flow-induced SUMOylation of ERK5 and p53 that leads to endothelial dysfunction and atherosclerosis.* Circ Res, 2013. **112**(6): p. 911-23.

77. Hay, R.T., *SUMO: a history of modification.* Mol Cell, 2005. **18**(1): p. 1-12.

78. Hay, R.T., *SUMO-specific proteases: a twist in the tail.* Trends Cell Biol, 2007. **17**(8): p. 370-6.

79. Hickey, C.M., N.R. Wilson, and M. Hochstrasser, *Function and regulation of SUMO proteases.* Nat Rev Mol Cell Biol, 2012. **13**(12): p. 755-66.

80. Cheng, J., et al., *SUMO-specific protease 1 is essential for stabilization of HIF1alpha during hypoxia.* Cell, 2007. **131**(3): p. 584-95.

81. Chiu, S.Y., et al., *SUMO-specific protease 2 is essential for modulating p53-Mdm2 in development of trophoblast stem cell niches and lineages.* PLoS Biol, 2008. **6**(12): p. e310.

82. Kang, X., et al., *SUMO-specific protease 2 is essential for suppression of polycomb group protein-mediated gene silencing during embryonic development.* Mol Cell, 2010. **38**(2): p. 191-201.

83. Martin, S., et al., *Emerging extranuclear roles of protein SUMOylation in neuronal function and dysfunction.* Nat Rev Neurosci, 2007. **8**(12): p. 948-59.

84. Mossessova, E. and C.D. Lima, *Ulp1-SUMO crystal structure and genetic*

analysis reveal conserved interactions and a regulatory element essential for cell growth in yeast. Mol Cell, 2000. **5**(5): p. 865-76.

85. Reverter, D. and C.D. Lima, *A basis for SUMO protease specificity provided by analysis of human Senp2 and a Senp2-SUMO complex.* Structure, 2004. **12**(8): p. 1519-31.

86. Reverter, D. and C.D. Lima, *Structural basis for SENP2 protease interactions with SUMO precursors and conjugated substrates.* Nat Struct Mol Biol, 2006. **13**(12): p. 1060-8.

87. Agbor, T.A., et al., *Small ubiquitin-related modifier (SUMO)-1 promotes glycolysis in hypoxia.* J Biol Chem, 2011. **286**(6): p. 4718-26.

88. Ran, Y., et al., *SENP2 negatively regulates cellular antiviral response by deSUMOylating IRF3 and conditioning it for ubiquitination and degradation.* J Mol Cell Biol, 2011. **3**(5): p. 283-92.

89. Hofker, M.H., *Introduction: the use of transgenic mice in biomedical research.* Methods Mol Biol, 2003. **209**: p. 1-8.

90. McPherron, A.C., A.M. Lawler, and S.J. Lee, *Regulation of skeletal muscle mass in mice by a new TGF-beta superfamily member.* Nature, 1997. **387**(6628): p. 83-90.

91. Barton-Davis, E.R., et al., *Viral mediated expression of insulin-like growth factor I blocks the aging-related loss of skeletal muscle function.* Proc Natl Acad Sci U S A, 1998. **95**(26): p. 15603-7.

92. Koretsky, A.P., *Insights into cellular energy metabolism from transgenic mice.* Physiol Rev, 1995. **75**(4): p. 667-88.

93. Brosnan, M.J., J.M. Halow, and A.P. Koretsky, *Manipulating creatine kinase activity in transgenic mice to study control of energy metabolism.* Biochem Soc Trans, 1991. **19**(4): p. 1010-4.

94. Richard, D., et al., *Energy balance and lipid metabolism in transgenic mice bearing an antisense GCR gene construct.* Am J Physiol, 1993. **265**(1 Pt 2): p. R146-50.

95. Bawa-Khalfe, T., et al., *SENP1 induces prostatic intraepithelial neoplasia through multiple mechanisms.* J Biol Chem, 2010. **285**(33): p. 25859-66.

96. Jacques, C., et al., *Two-step differential expression analysis reveals a new set of genes involved in thyroid oncocytic tumors.* J Clin Endocrinol Metab, 2005. **90**(4): p. 2314-20.

97. Cheng, J., et al., *Role of desumoylation in the development of prostate cancer.* Neoplasia, 2006. **8**(8): p. 667-76.

98. Kim, E.Y., et al., *Enhanced desumoylation in murine hearts by overexpressed SENP2 leads to congenital heart defects and cardiac dysfunction.* J Mol Cell Cardiol, 2012. **52**(3): p. 638-49.

99. Kaikkonen, S., et al., *SUMO-specific protease 1 (SENP1) reverses the hormone-augmented SUMOylation of androgen receptor and modulates gene responses in prostate cancer cells.* Mol Endocrinol, 2009. **23**(3): p.

292-307.

100. Abdel-Hafiz, H.A. and K.B. Horwitz, *Control of progesterone receptor transcriptional synergy by SUMOylation and deSUMOylation.* BMC Mol Biol, 2012. **13**: p. 10.

101. Ellis, J.M., et al., *Adipose acyl-CoA synthetase-1 directs fatty acids toward beta-oxidation and is required for cold thermogenesis.* Cell Metab, 2010. **12**(1): p. 53-64.

102. McGarry, J.D. and N.F. Brown, *The mitochondrial carnitine palmitoyltransferase system. From concept to molecular analysis.* Eur J Biochem, 1997. **244**(1): p. 1-14.

103. Kleiner, S., et al., *PPAR{delta} agonism activates fatty acid oxidation via PGC-1{alpha} but does not increase mitochondrial gene expression and function.* J Biol Chem, 2009. **284**(28): p. 18624-33.

104. Oropeza, D., et al., *PGC-1 coactivators in beta-cells regulate lipid metabolism and are essential for insulin secretion coupled to fatty acids.* Mol Metab, 2015. **4**(11): p. 811-22.

105. Liang, H. and W.F. Ward, *PGC-1alpha: a key regulator of energy metabolism.* Adv Physiol Educ, 2006. **30**(4): p. 145-51.

106. Chen, S.C., et al., *Sumoylation-promoted enterovirus 71 3C degradation correlates with a reduction in viral replication and cell apoptosis.* J Biol Chem, 2011. **286**(36): p. 31373-84.

107. Tatham, M.H., et al., *RNF4 is a poly-SUMO-specific E3 ubiquitin ligase required for arsenic-induced PML degradation.* Nat Cell Biol, 2008. **10**(5): p. 538-46.

108. van Hagen, M., et al., *RNF4 and VHL regulate the proteasomal degradation of SUMO-conjugated Hypoxia-Inducible Factor-2alpha.* Nucleic Acids Res, 2010. **38**(6): p. 1922-31.

109. Hevener, A.L., et al., *Muscle-specific Pparg deletion causes insulin resistance.* Nat Med, 2003. **9**(12): p. 1491-7.

110. Norris, A.W., et al., *Muscle-specific PPARgamma-deficient mice develop increased adiposity and insulin resistance but respond to thiazolidinediones.* J Clin Invest, 2003. **112**(4): p. 608-18.

국문초록

SUMOylation은 단백질의 가역적인 posttranscriptional modification 중의 하나이다. 단백질이 SUMOylation이 되면 굉장히 많은 기능을 갖게 된다. 기존 연구에 의하면, SUMOylation에 의해서 단백질의 안정성, 전사조절 등에 중요한 역할을 한다고 보고되어있다. 일반적으로 SUMOylatione 된 단백질은 deSUMOylating 단백질인 SENPs 의해서 deSUMOylation이 된다. 그러나 에너지 대사에 있어서SENPs의 생리학적인 기능은 현재까지 많은 연구가 되어 있지 않다. 따라서 저자는 본 연구를 통해 생쥐의 골격근 세포 주 및 동물 모델을 통해 SENP2가 지방산 대사에 어떠한 역할을 하는지에 대해 연구하였다.

C2C12 myotubes에 palmitate를 처리하면 TLR4-Myd88-NF-kB 신호전달경로를 통해 SENP2의 발현을 증가시킨다. 이러한 SENP2의 증가는 PPARδ와 PPARγ의 deSUMOylation을 통해 지방산 대사에 중요한 역할을 담당하는 유전자인 CPT1b와

ACLS1의 발현 양을 증가 시킴으로써 지방산 산화를 활성화시킨다. PPARδ와 PPARγ의 발현을 억제시켰을 경우에는 palmitate에 의한 SENP2, CPT1b 그리고 ACLS1의 발현 증가가 관찰되지 않았으며, 지방산 산화까지도 증가되지 않았다.

C2C12 myotubes에 SENP2를 과 발현 시키면 지방산 산화가 증가하였고 관련 유전자인 CPT1b와 ACLS1의 발현양도 증가하였다. SENP2가 골격근 특이적으로 과 발현 되어 있는 생쥐와 그렇지 않은 일반 생쥐를 동일하게 고지방식을 먹였을 경우 골격근에 SENP2가 특이적으로 과 발현 되어 있는 생쥐는 일반 쥐에 비해 몸무게가 감소하였으며 몸 전체의 지방비율도 현저히 감소하였다. 그리고 당 부하검사와 인슐린 내성 시험에서도 SENP2 형질전환 생쥐에서 당 부하와 인슐린 내성이 개선되는 효과가 있음을 관찰 할 수 있었다. 또한, SENP2 형질전환 생쥐에서 골격근 내 지방산 산화가 많이 일어나고 미토콘드리아의 양 또한 증가되어 있었다. 더 나아가 골격근 내에 SENP2 단백질이 과 발현되면 인슐린 신호전달에 관여하는 단백질인 IRS1과 AKT의 인산화 수준이 증가되는 것을 확인하였다.

이러한 결과를 통해 골격근 내 지방산 대사 및 미토콘드리아 활성에 있어 SENP2가 중요한 역할을 함을 알 수 있다. 그리고 한 발 더 나아가 SENP2가 비만과 관련된 대사 증후군에 새로운 치료제로서의 표적이 될 수도 있을 것이다.

주요어 : SENP2, deSUMOylation, 지방산 대사, 비만, 골격근

학 번 : 2009-30599